Neutron Star Equation of State after the GW170817 event

David E. Álvarez Castillo
Joint Institute for Nuclear Research
Dubna, Russia

INSTITUTO DE CIENCIAS NUCLEARES
UNAM
May 31, 2019

JINR
DUBNA

PHAROS
THE MULTI-MESSENGER PHYSICS AND ASTROPHYSICS OF NEUTRON STARS

comp star

Outline

- A brief introduction to the neutron star equation of state.
- The interplay of the symmetry energy and DUrca cooling.
- Astrophysics measurements of compact stars: multi-messenger astronomy & the GW170817 event.
- The compact star mass twins case.
- Astrophysical implications and perspectives.

Double Neutron Stars and Millisecond Pulsars

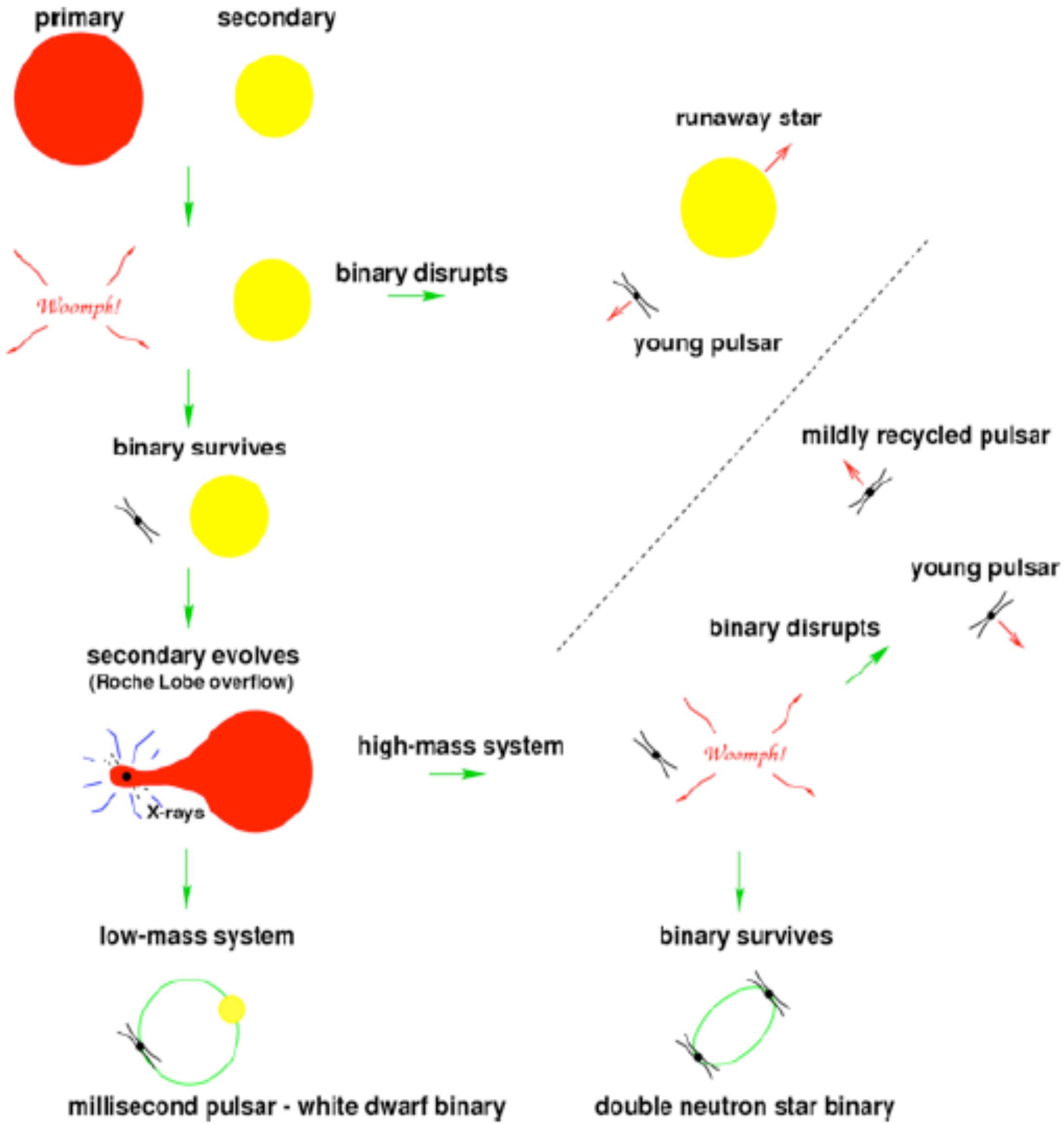

Pulse shapes and el.-magn. spectrum

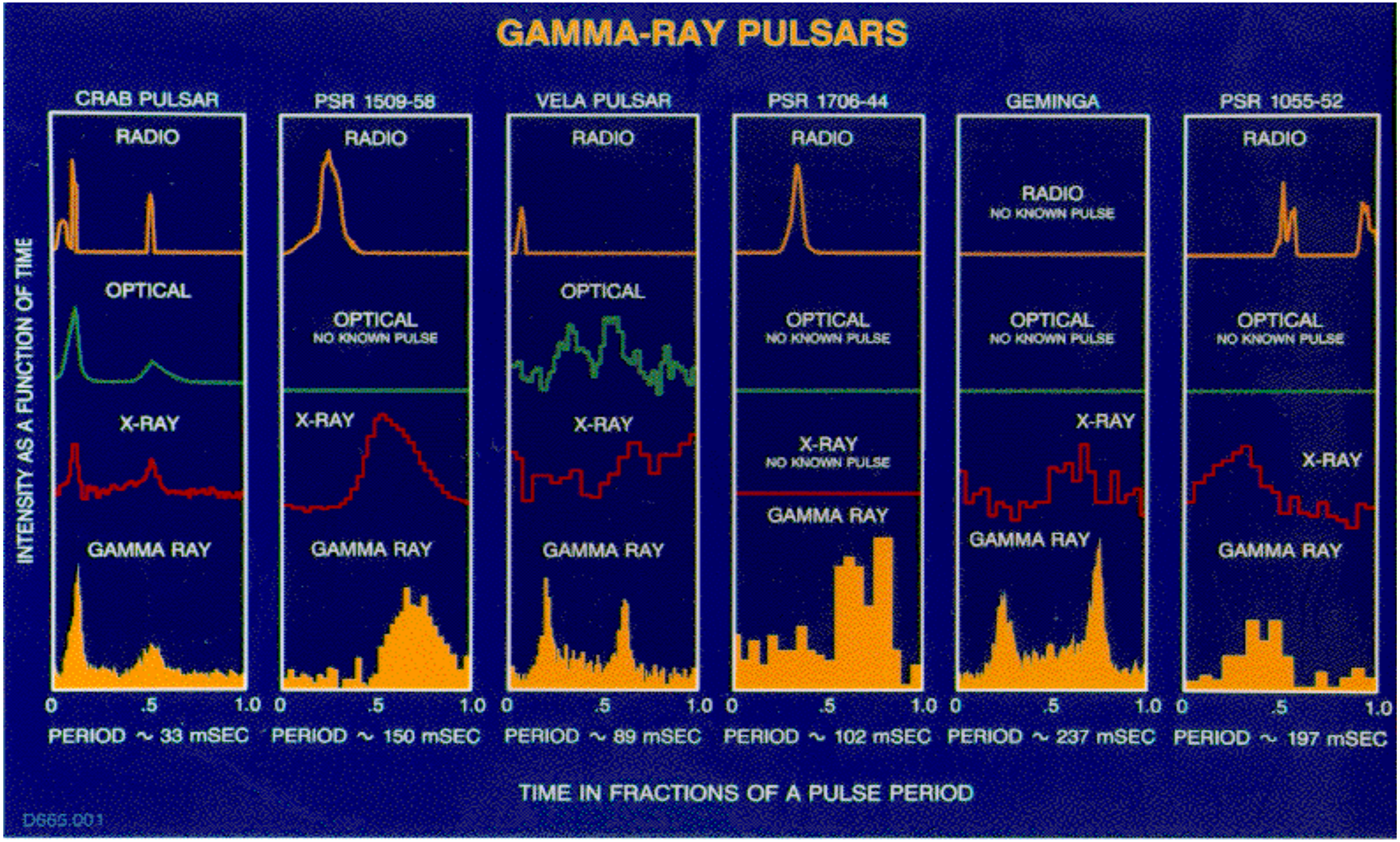

Statistics of Pulsars

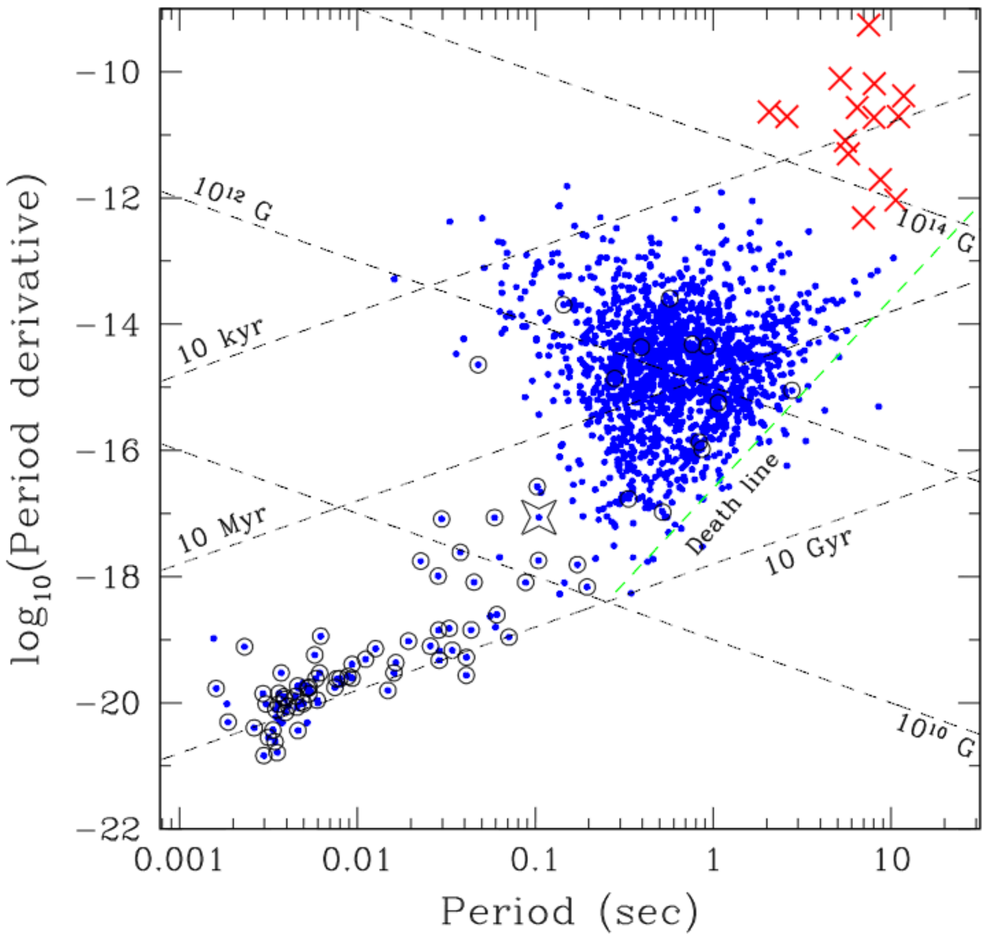

Magnetars:
$B > 10^{15}$ Gauss

Young pulsars:
$P < 1$ sec
$B \sim 10^{12}$ Gauss

Recycled (old) Pulsars:
$P \sim$ few milliseconds
$B \sim 10^{8}$ Gauss

Superdense objects – what is inside?

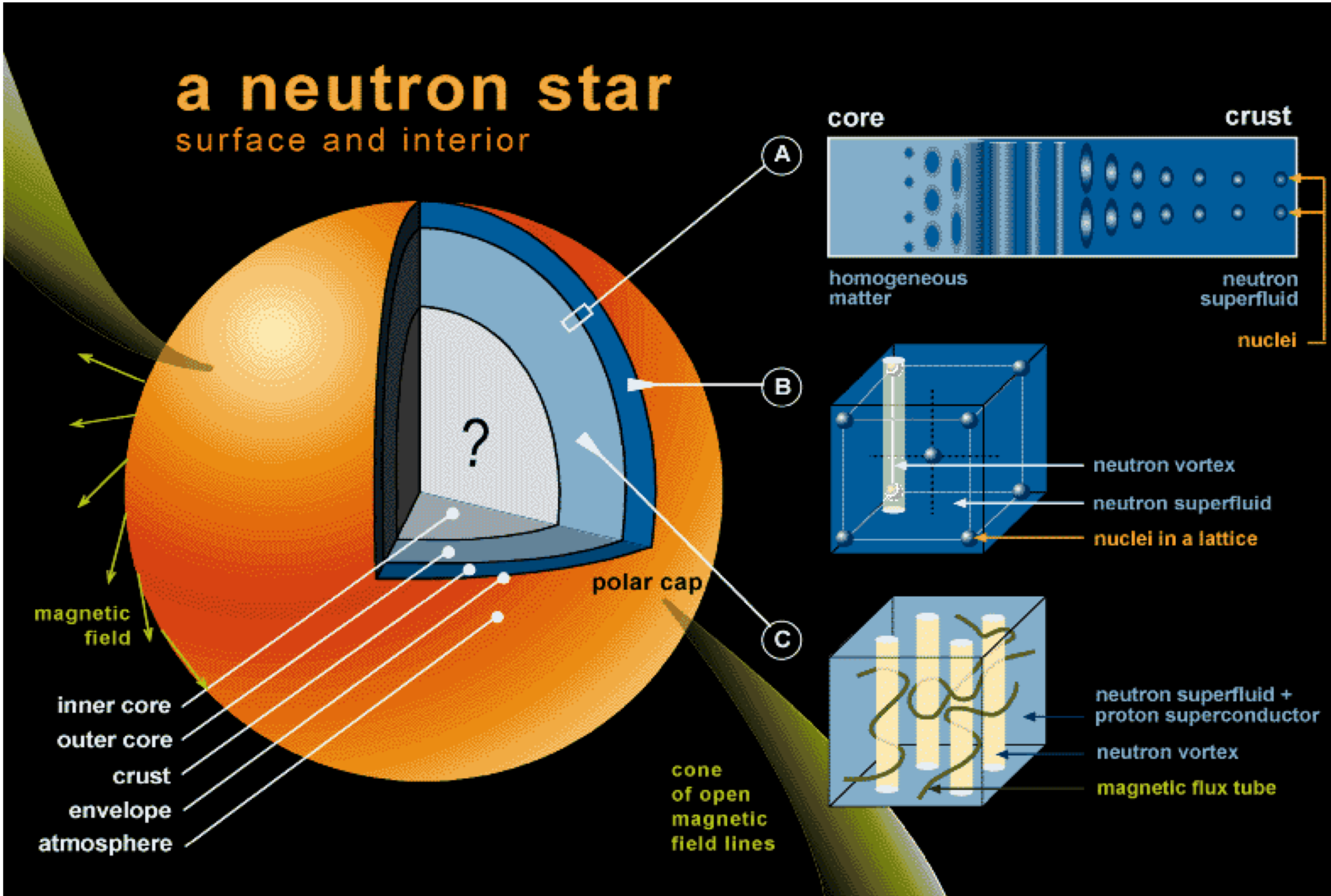

Superdense objects – what is inside?

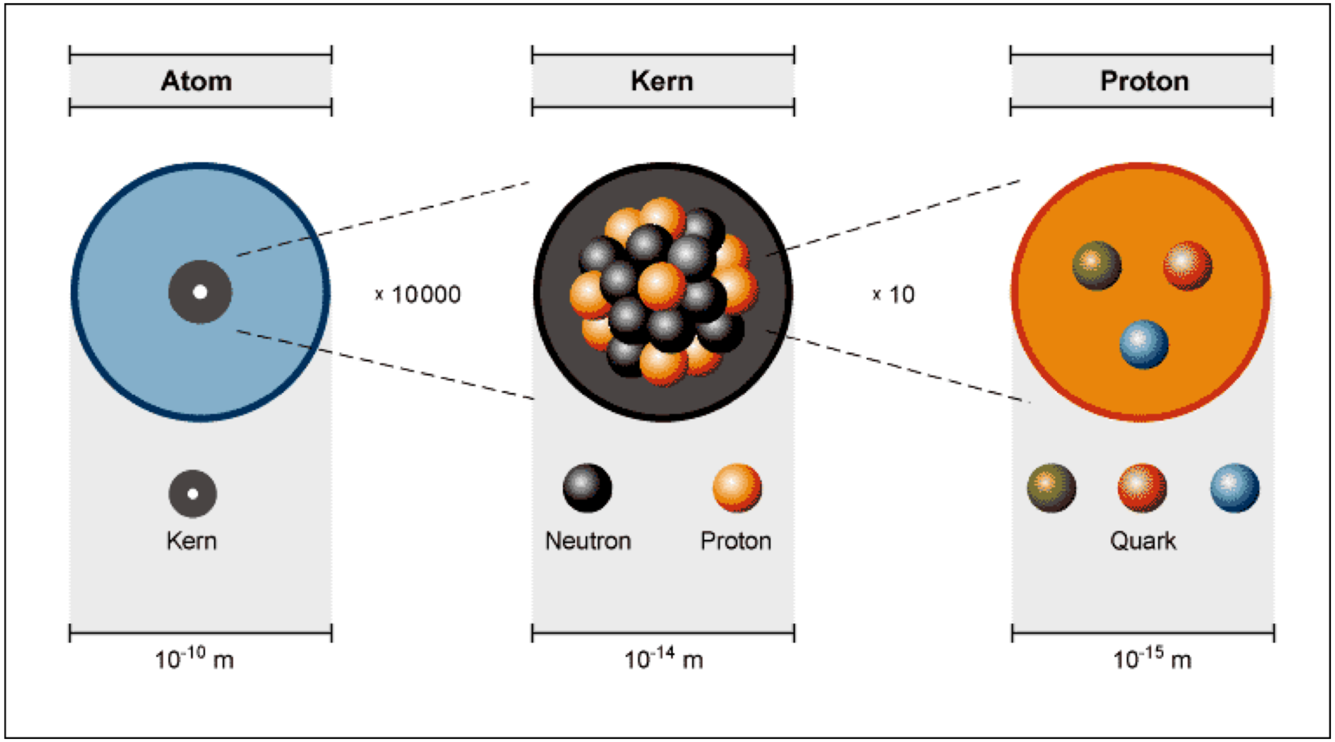

Nucleus, A nucleons: R_A=1.2 10^{-13} cm $A^{1/3}$; ρ_0=A1.67 10^{-24} g/(4π/3 $R_A^{\ 3}$)= 2.3 10^{14} g/cm^3

Neutron star: R= 10 km; ρ= 2 Mo/(4π/3 R^3) = 4 10^{33} g/(4 10^{18} cm^3)= 10^{15} g/cm^3 = 4 ρ_0

Superdense objects – what is inside?

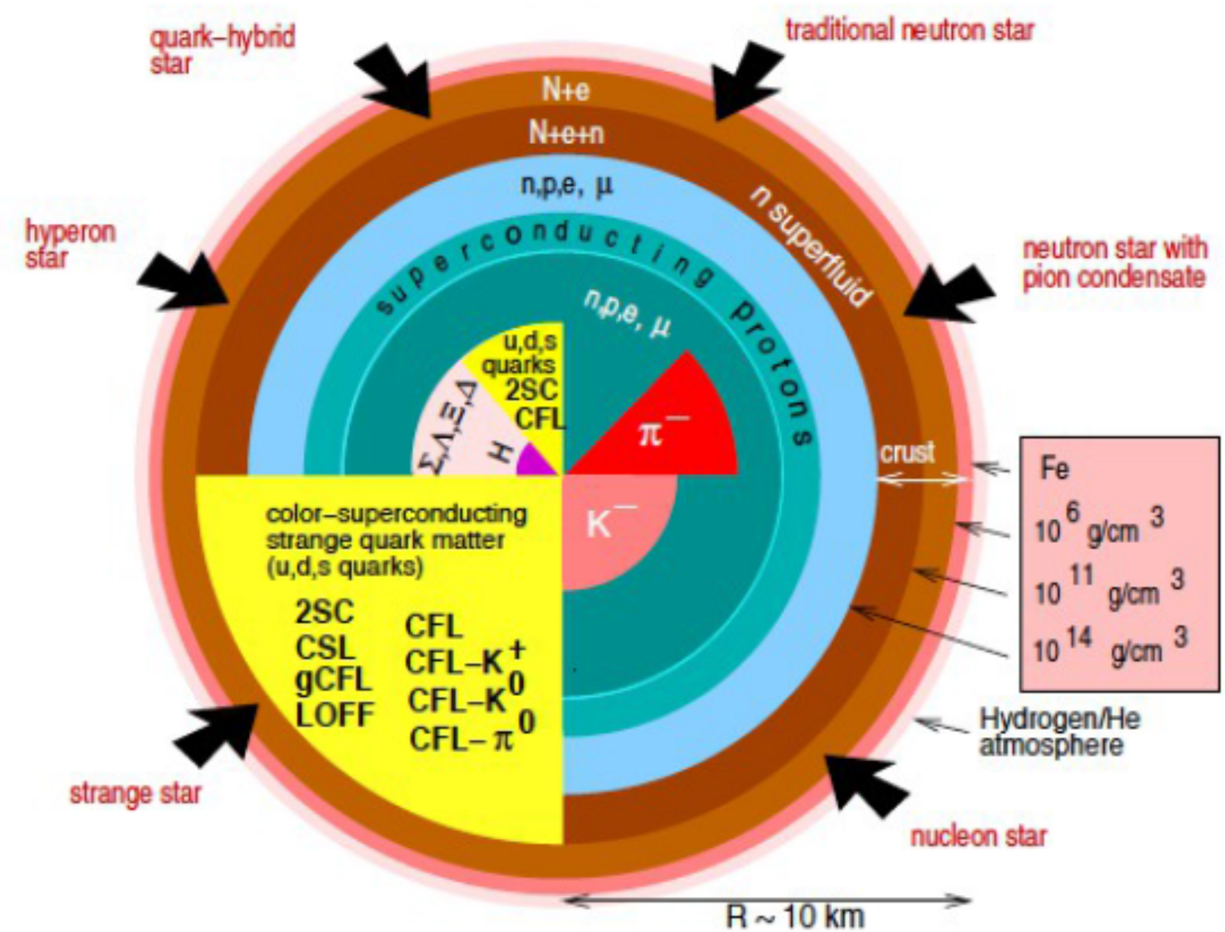

Nuclear Matter

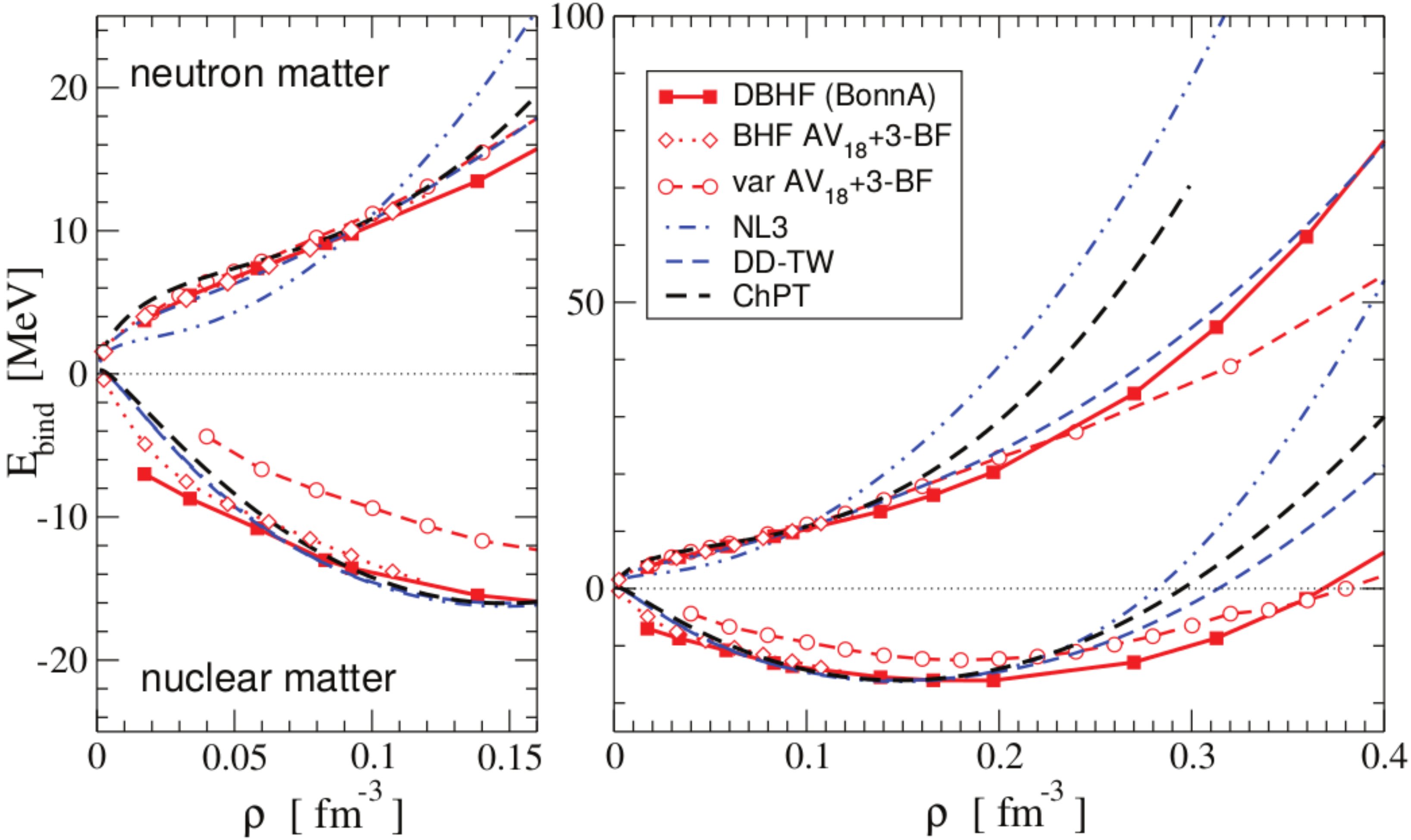

C. Fuchs, H.H. Wolter, EPJA 30(2006)5

Flow Constraint

Klaehn et al. PhysRev C74 (2006)
P. Danielewicz, R. Lacey and W.G. Lynch, Science 298, 1592 (2002)

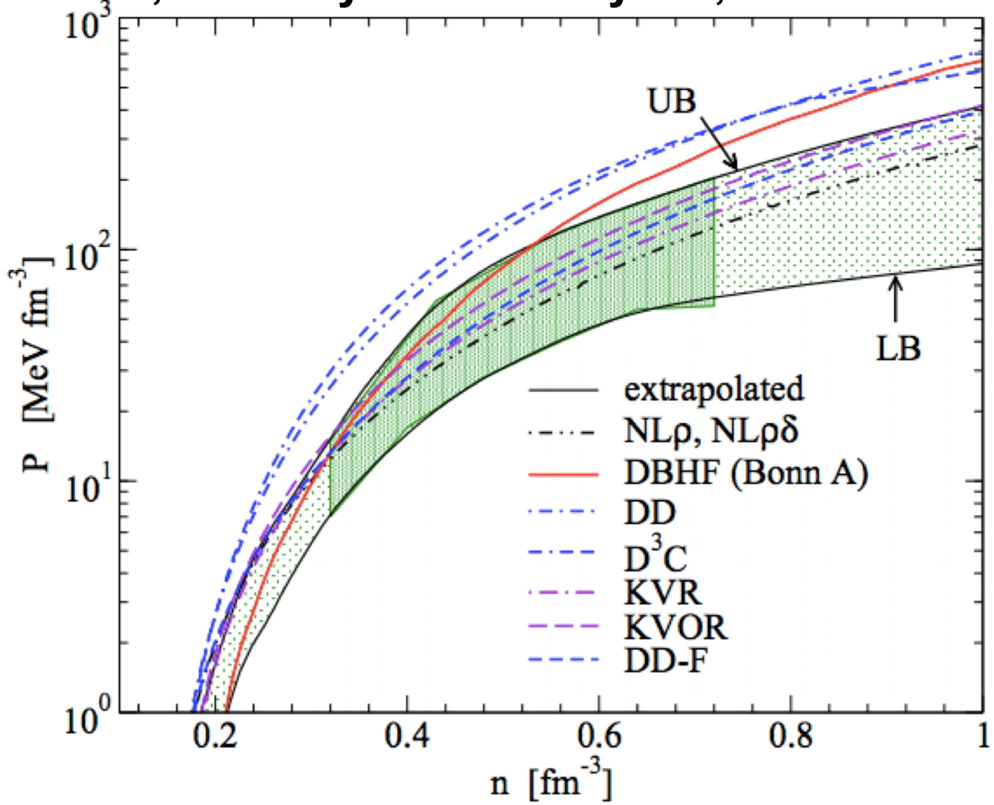

FIG. 6: Pressure region consistent with experimental flow data in SNM (dark shaded region). The light shaded region extrapolates this region to higher densities within an upper (UB) and lower border (LB).

Nuclear Symmetry Energy

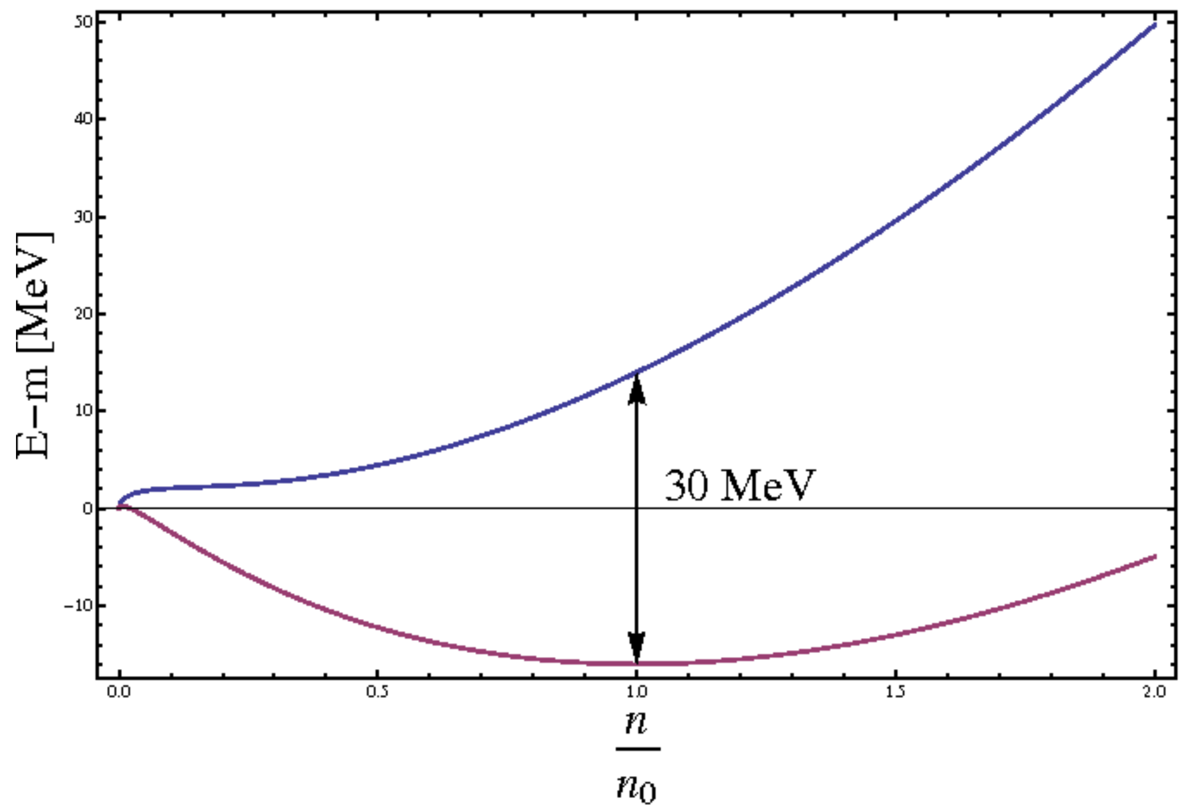

is the difference between symmetric nuclear matter and pure neutron matter:

$$E(n,x) = E(n, x = 1/2) + E_s(n) * \alpha^2(x) + E_q(n) * \alpha^4(x) + O(\alpha^6(x))$$

where $\alpha = 1 - 2x$

Measuring the symmetry energy

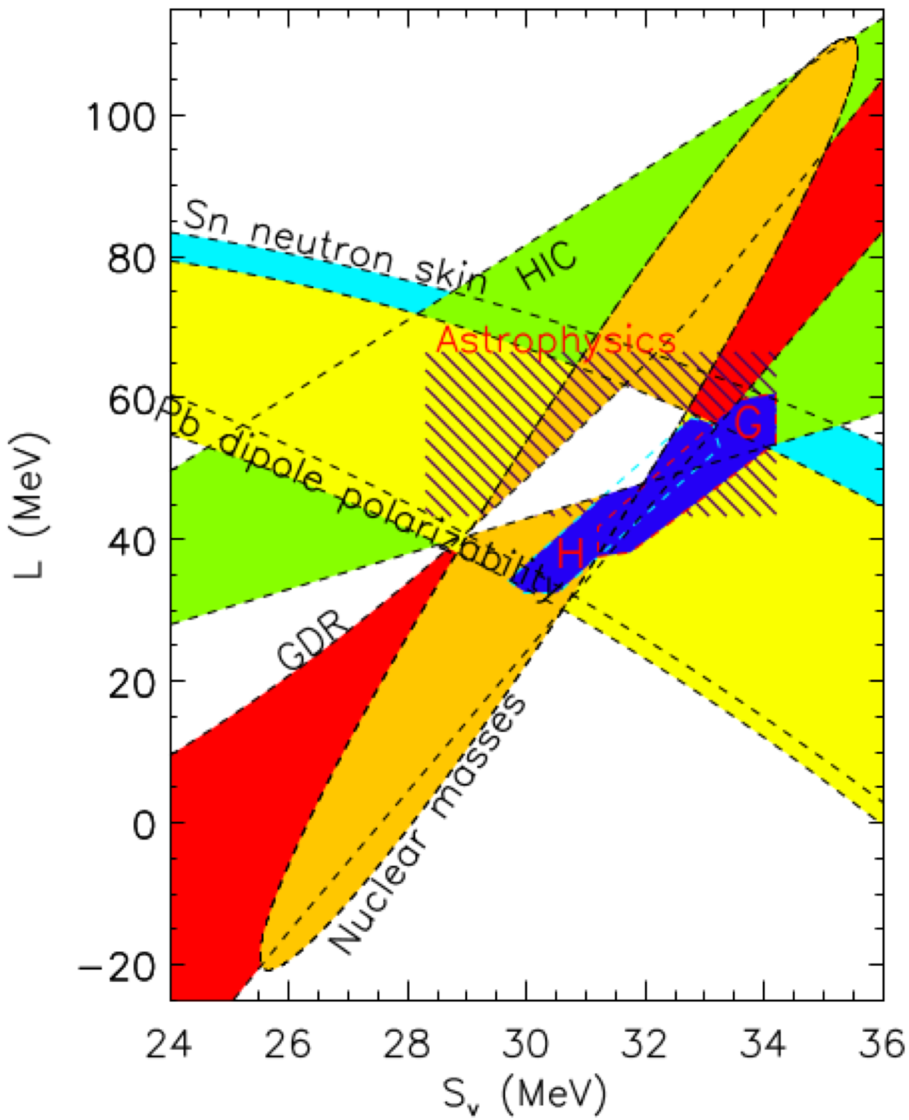

Lattimer and Lim (2013) ApJ 771 51

Neutron Star Equation of State

The energy per nucleon in neutron star core matter is given by:

$$\begin{aligned} E_{\rm tot}(n, \{x_i\}) &= E_{\rm b}(n, x_p) + E_{\rm lep}(n, x_e, x_\mu) \ , \\ E_{\rm b}(n, x_p) &= E_0(n) + S(n, x_p) \\ E_{\rm lep}(n, x_e, x_\mu) &= E_e(n, x_e) + E_\mu(n, x_\mu) \ , \end{aligned}$$

where $n = n_p + n_n$ is the total baryon density and $x_i = n_i/n$, $i = p, e, \mu$ are the fractions of protons, electrons and muons, respectively. The baryonic part is very well described by the parabolic approximation w.r.t. the asymmetry

$$\alpha = \frac{n_n - n_p}{n_n + n_p} = 1 - 2x_p,$$

resulting in $S(n, x_p) = (1 - 2x_p)^2 E_s(n)$. The leptonic contribution is a sum of the Fermi gas expressions for the contributing leptons $l = e, \mu$

$$E_l(n, x_l) = \frac{1}{n}\frac{p_{F,l}^4}{4\pi^2}\left[\sqrt{1 + z_l^2}\left(1 + \frac{z_l^2}{2}\right) - \frac{z_l^4}{2}\text{Arsinh}\left(\frac{1}{z_l}\right)\right] \ ,$$

where $z_l = m_l/p_{F,l}$. For massless leptons ($z_l \to 0$), this expression goes over to

$$E_l(n, x_l)\big|_{m_l=0} = \frac{1}{n}\frac{p_{F,l}^4}{4\pi^2} = \frac{3}{4}\left(3\pi^2 n\right)^{1/3} x_l^{4/3} \ .$$

Charge neutrality and β-equillibrium

Under neutron star conditions charge neutrality holds,

$$x_p = x_e + x_\mu \ .$$

The $\beta-$ equilibrium with respect to the weak interaction processes $n \to p + e^- + \bar{\nu}_e$ and $p + e^- \to n + \nu_e$ (and similar for muons), for cold neutron stars (temperature T below the neutrino opacity criterion $T < T_\nu \sim 1$ MeV) implies

$$\mu_n - \mu_p = \mu_e = \mu_\mu \ .$$

The chemical potentials are defined as

$$\mu_i = \frac{\partial \varepsilon_i}{\partial n_i} = \frac{\partial}{\partial x_i} E_i(n, \{x_j\}) \ , \quad i, j = n, p, e, \mu \ ,$$

where $\varepsilon_i = n \ E_i(n, \{x_j\})$ is the partial energy density of species i in the system. From the above equations:

$$\mu_e = 4(1-2x)E_s(n) \ .$$

Since electrons in neutron star interiors are ultrarelativistic,

$$\mu_e = \sqrt{p_{F,e}^2 + m_e^2} \approx p_{F,e}, \text{ and } p_{F,e} = (3\pi^2 n_e)^{1/3} = (3\pi^2 n)^{1/3}(x - x_\mu)^{1/3} \ ,$$

$$\frac{x - x_\mu}{(1-2x)^3} = \frac{64 E_s^3(n)}{3\pi^2 n} \ , \qquad (x - x_\mu)^{2/3} - x_\mu^{2/3} = \frac{m_\mu^2}{(3\pi^2 n)^{2/3}} \ .$$

The total pressure is then given as $P(n) = n^2 \left(\frac{\partial E_{\rm tot}}{\partial n} \right)$.

Compact Star Sequences
(M-R ⇔ EoS)

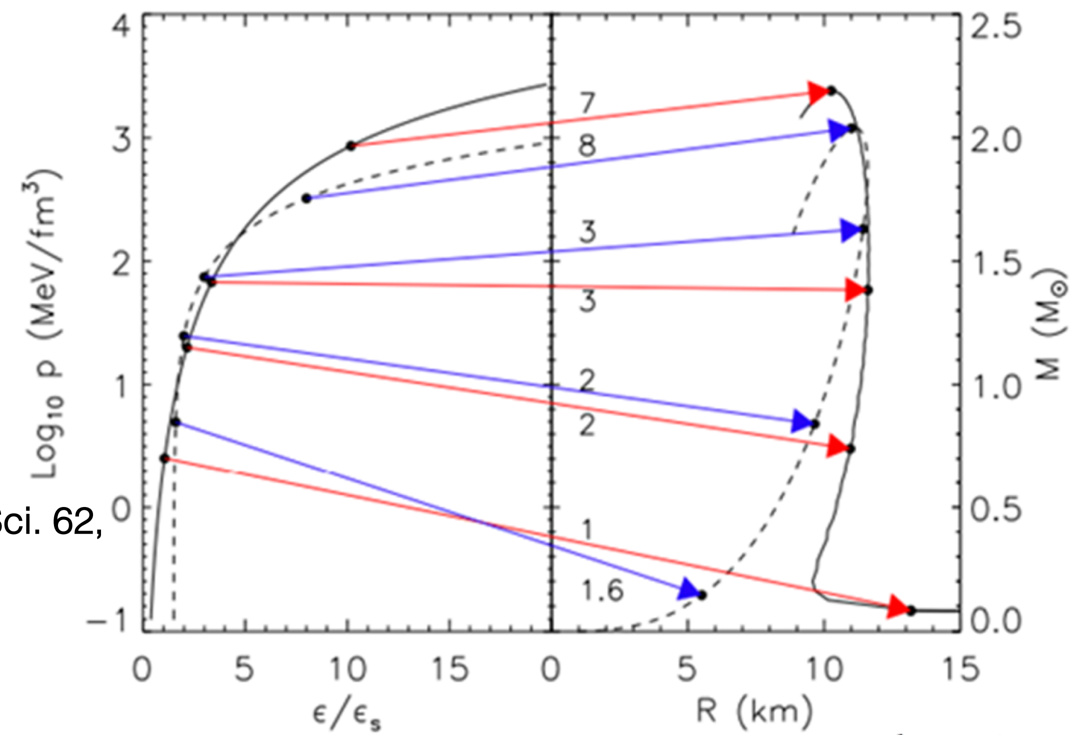

Lattimer,
Annu. Rev. Nucl. Part. Sci. 62, 485 (2012)
arXiv: 1305.3510

- TOV Equations

$$\frac{dp}{dr} = -\frac{(\varepsilon + p/c^2)G(m + 4\pi r^3 p/c^2)}{r^2(1 - 2Gm/rc^2)}$$

$$\frac{dm}{dr} = 4\pi r^2 \varepsilon$$

- Equation of State (EoS)

$$p(\varepsilon)$$

PSR J1614-2230

A precise AND large mass measurement

Shapiro delay:

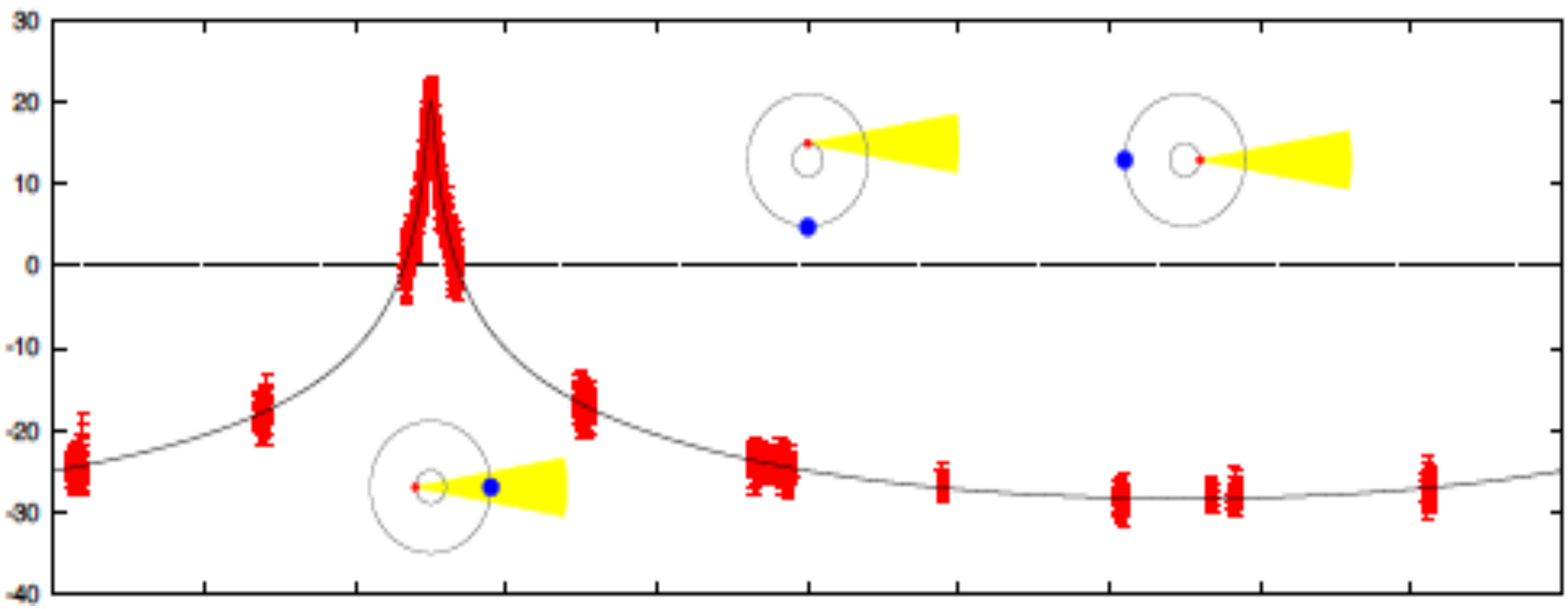

Massive Neutron Stars

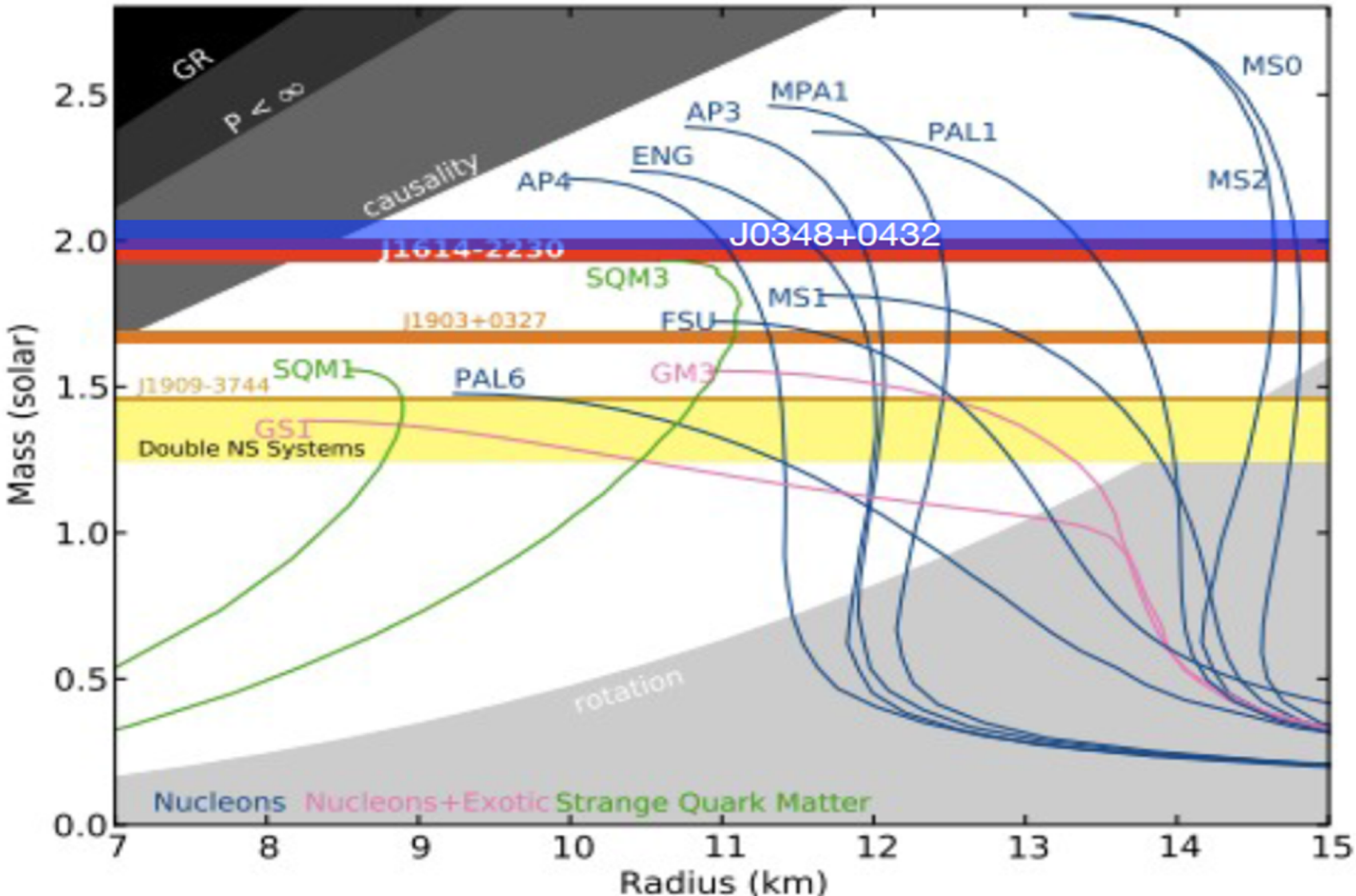

Massive Neutron Stars

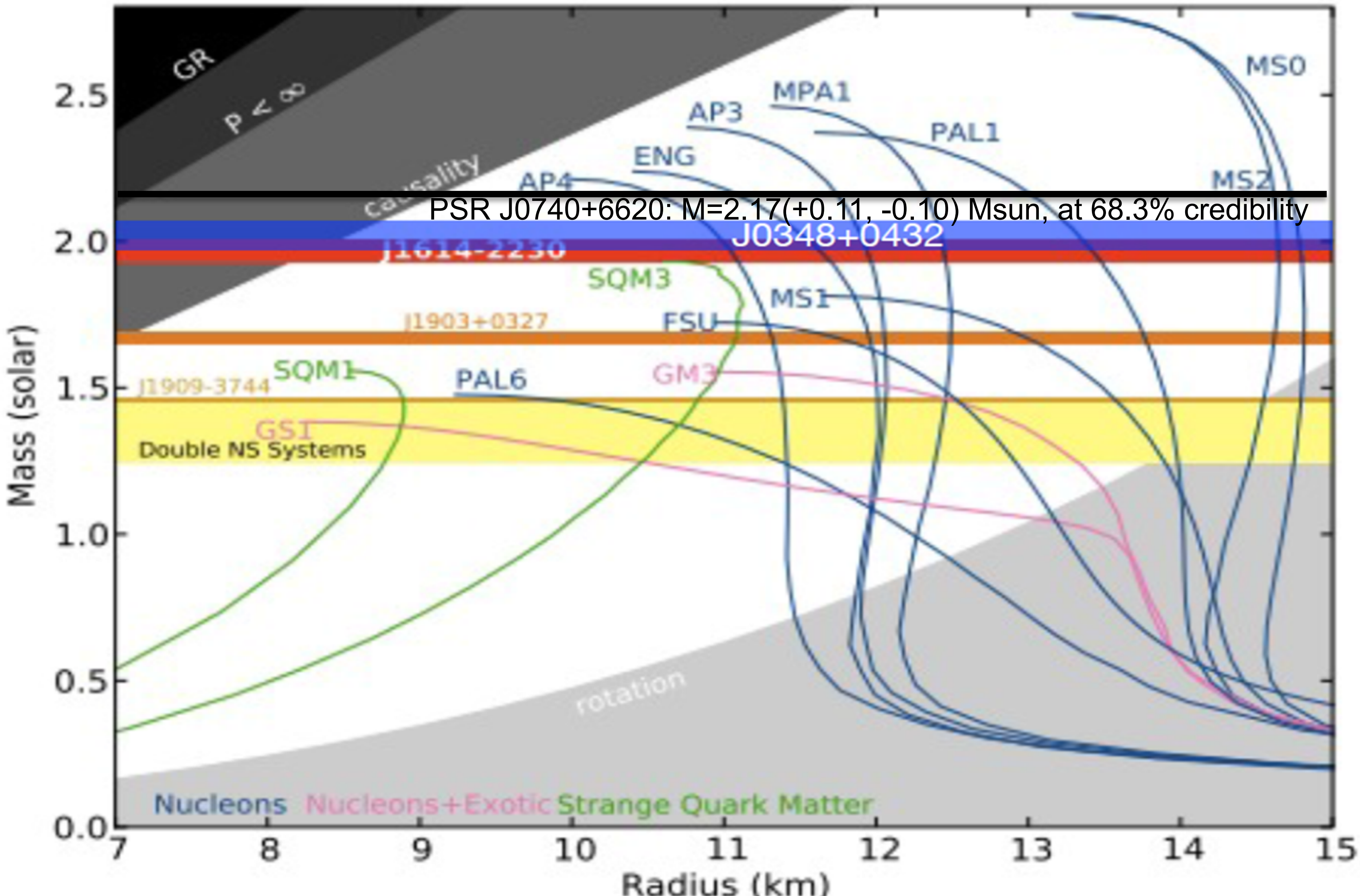

Symmetry energy effects

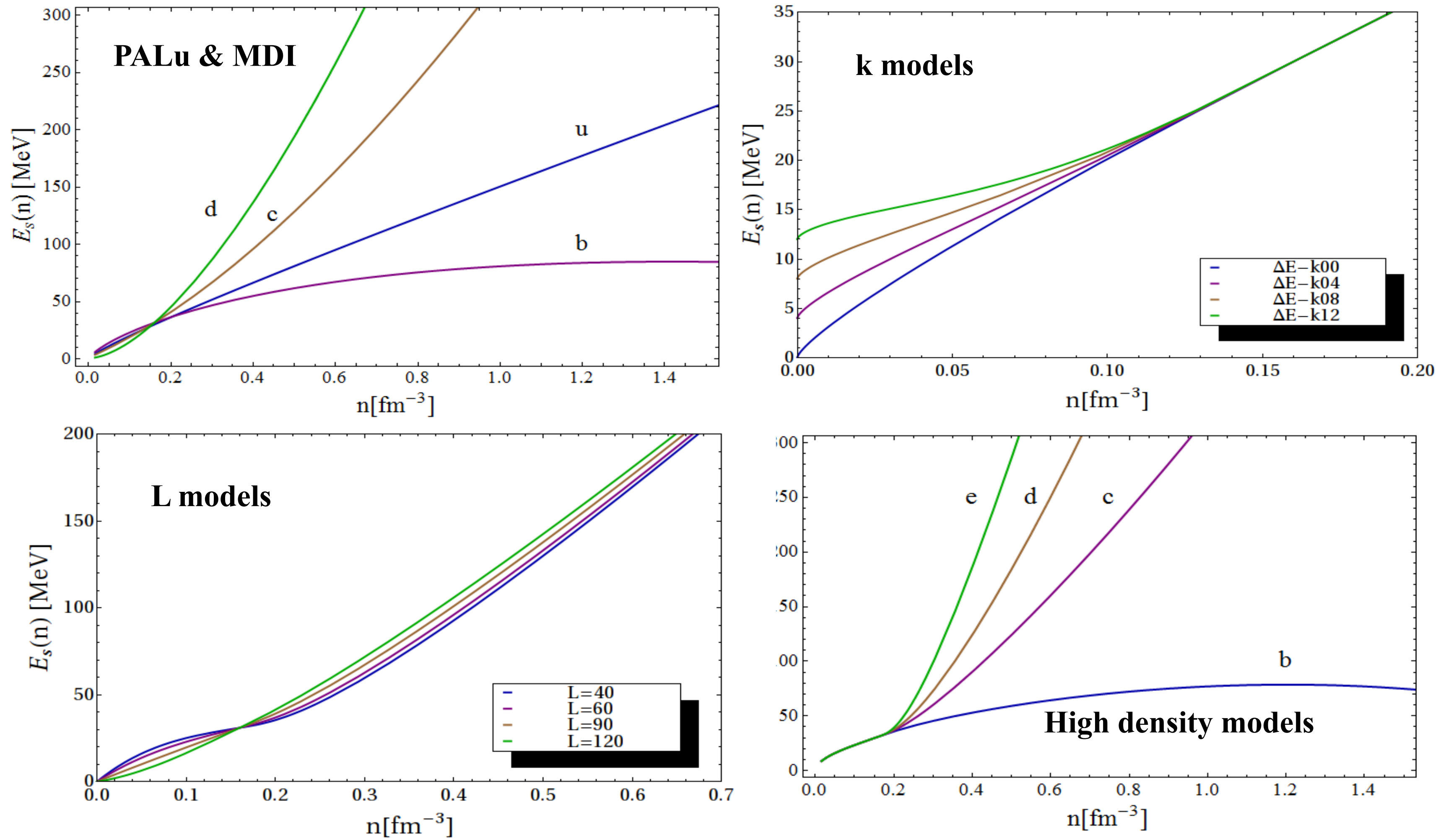

S. Kubis and D. E. Alvarez-Castillo - arXiv:1205.6368

Symmetry energy effects

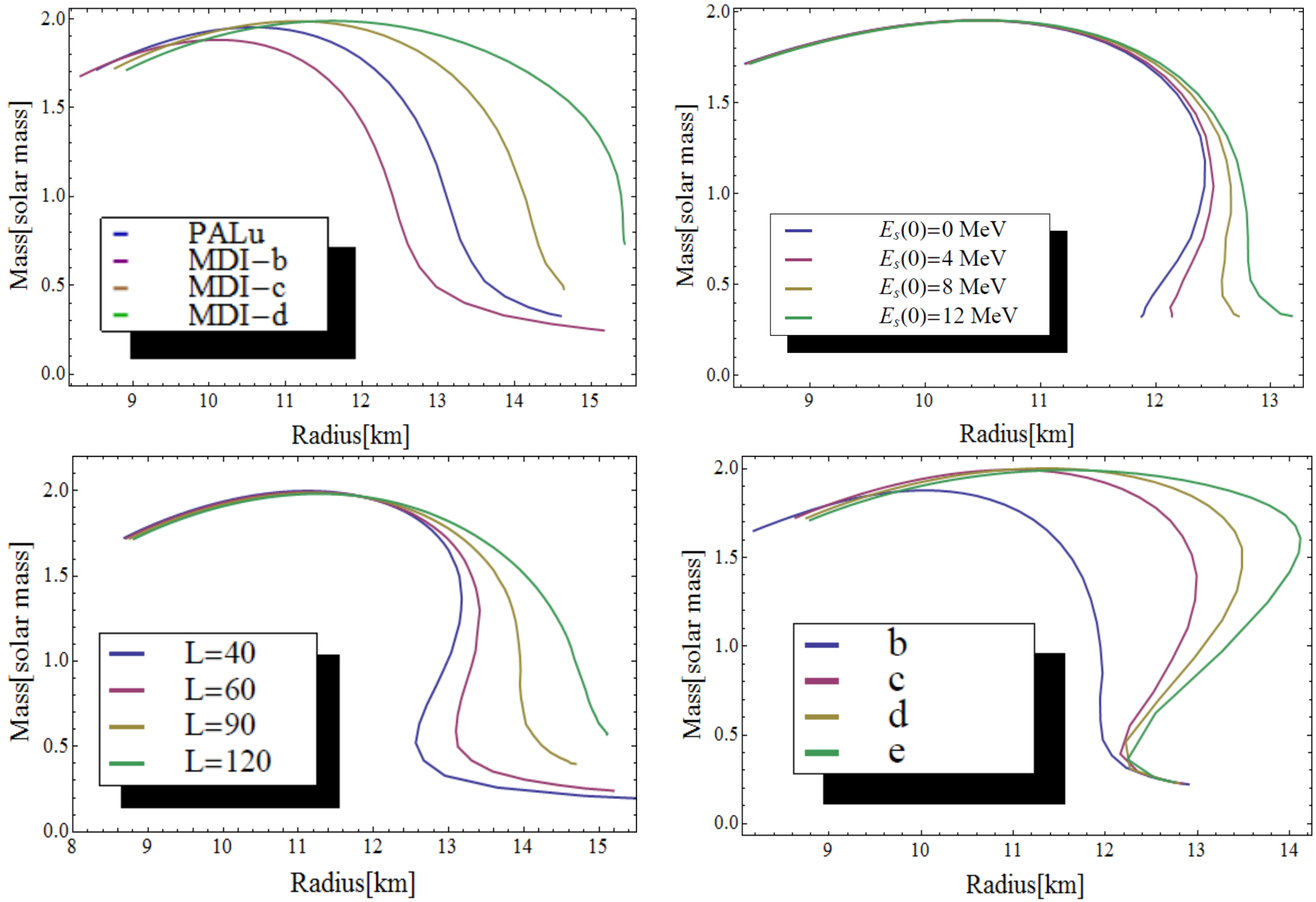

S. Kubis and D. E. Alvarez-Castillo - arXiv:1205.6368

Neutron Star Cooling Processes

Process Name	Process	Emissivity Q_ν (erg cm^{-3} s^{-1})	Reference
Bremsstrahlung	$n+n \to n+n+\nu_e+\bar{\nu}_e$ $n+p \to n+p+\nu_e+\bar{\nu}_e$ $p+p \to p+p+\nu_e+\bar{\nu}_e$	$\simeq 10^{19} T_9^8$	Page, Geppert and Weber [92]
Modified Urca	$n+n \to n+p+e^-+\bar{\nu}_e$ $n+p+e^- \to n+n+\nu_e$	$\simeq 10^{20} T_9^8$	Friman and Maxwell [93]
Direct Urca	$n \to p+e^-+\bar{\nu}_e$ $p+e^- \to n+\nu_e$	$\simeq 10^{27} T_9^6$	Lattimer et al. [94]
Quark Urca	$d \to u+e^-+\bar{\nu}_e$ $u+e^- \to d+\nu_e$	$\simeq 10^{26} \alpha_c T_9^6$	Iwamoto [95]
Kaon Condensate	$n+K^- \to n+e^-+\bar{\nu}_e$ $n+e^- \to n+K^-+\nu_e$	$\simeq 10^{24} T_9^6$	Brown et al. [96]
Pion Condensate	$n+\pi^- \to n+e^-+\bar{\nu}_e$ $n+e^- \to n+\pi^-+\nu_e$	$\simeq 10^{26} T_9^6$	Maxwell et al. [97]

Direct Urca is the fastest cooling process.
Threshold for onset: $p_{F,n} < p_{F,p+} p_{F,e}$. For electrons only then $x_{DU}=1/9$.

DUrca Process Constraint

E_s plays an important role in determination of the activation of the direct Urca (DU) cooling process

$$n \to p + e + \bar{\nu}_e.$$

If the central density in a neutron star exceeds the critical value which allows the DU process to operate then this process triggers a dramatic drop of the core temperature due to rapid energy loss by neutrino emission. This process can therefore not be operative in typical neutron stars as we do observe cooling neutron stars much older than the typical transport timescale ($\sim$ 1000 years) with surface temperatures that are not compatible with DU cooling.

The DU threshold condition is derived from the triangle inequality for the Fermi momenta of neutron, proton and electron (neutrinos are neglected):

$$n_n^{1/3} < n_p^{1/3} + n_e^{1/3} \ ,$$

which can be formulated in terms of proton and muon fractions as

$$(1 - x)^{1/3} < x^{1/3} + (x - x_\mu)^{1/3} \ .$$

Below the muon threshold $x^{\mathrm{DU}} = 1/9 = 11.1$.

D. E. Alvarez-Castillo, D. Blaschke and T. Klahn. (2016)
arXiv: 1604.08575

DUrca Process Constraint

E_s	n_{DU}[fm^{-3}]	n_c[fm^{-3}]				
		1.25	1.40	1.60	1.80	2.00
DD2-	-	0.331	0.352	0.385	0.423	0.472
DD2	-	0.331	0.354	0.387	0.426	0.478
DD2+	-	0.325	0.349	0.384	0.425	0.479
DD2++	0.354	0.314	0.339	**0.375**	**0.416**	**0.469**

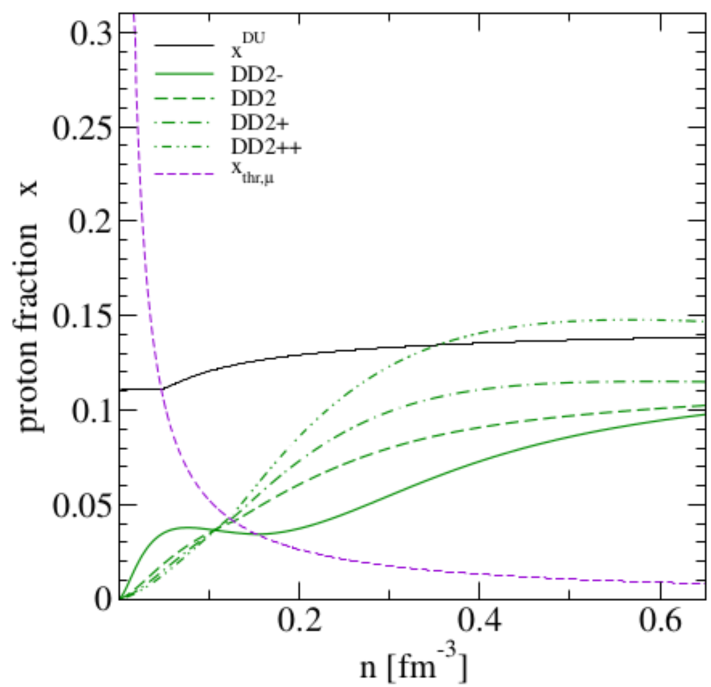

D. E. Alvarez-Castillo, D. Blaschke and T. Klahn. (2016)
arXiv: 1604.08575

Symmetry energy Conjecture

Klaehn et al. PhysRev C74 (2006)

PHYSICAL REVIEW C **74**, 035802 (2006)

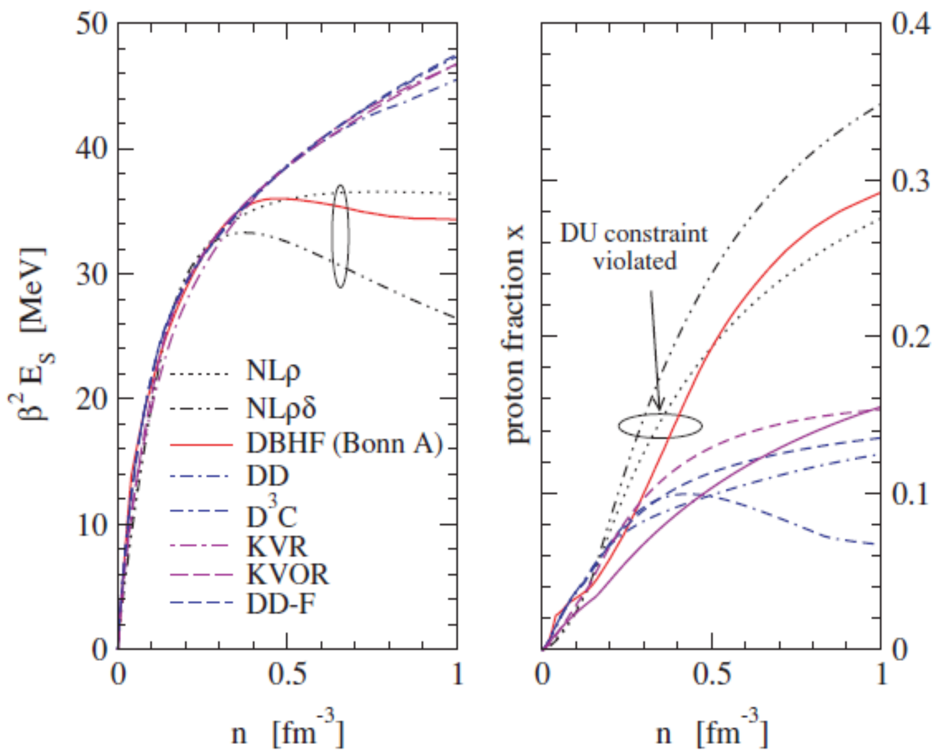

FIG. 7. (Color online) Density dependence of the asymmetry contribution to the energy per particle (left panel) and of the proton fraction (right panel) in NSM. Encircled curves correspond to EoSs that violate the DU-constraint.

Nuclear Symmetry Energy

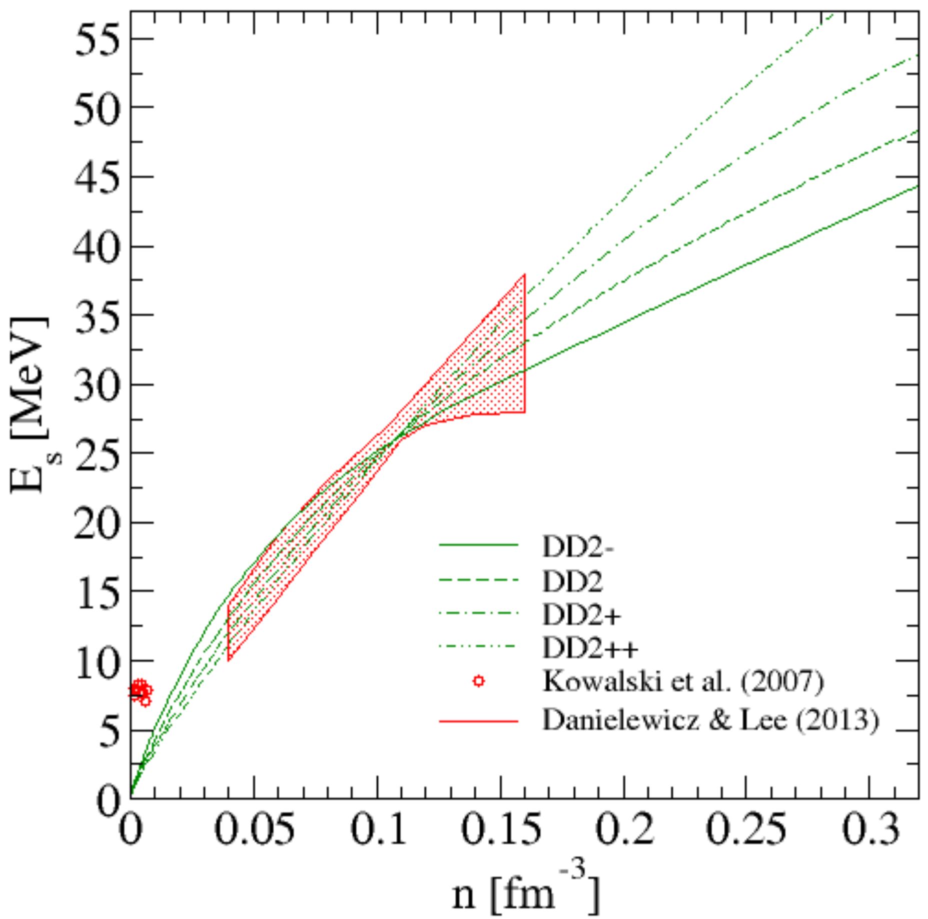

$E_s(n)$	Parametrization		$\Gamma_\rho(n_{\text{sat}})$	a_ρ
Stiff	DD2+	DD2F+	3.806504	0.342181
Medium	DD2	DD2F	3.626940	0.518903
Soft	DD2−	DD2F−	3.398486	0.742082

S. Typel, Phys. Rev. C 89, 064321 (2014)

Universal symmetry energy contribution

D. E. Alvarez-Castillo, D. Blaschke and T. Klahn. (2016)
arXiv: 1604.08575

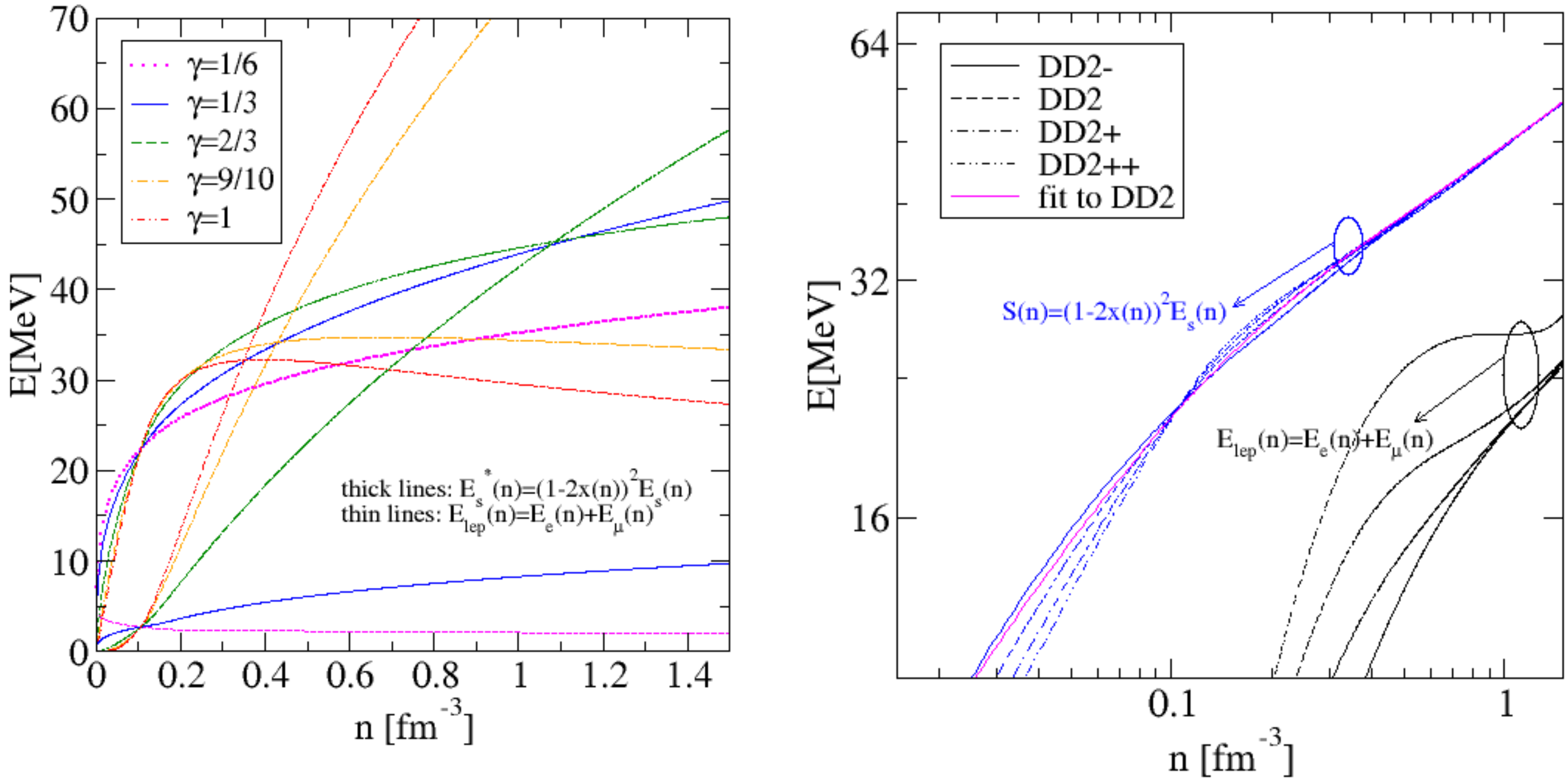

The symmetry energy contribution to the neutron star EoS behaves universal only then E_{sym} and therefore the proton fraction x is bounded (right panel)!

Predictions for neutron stars properties

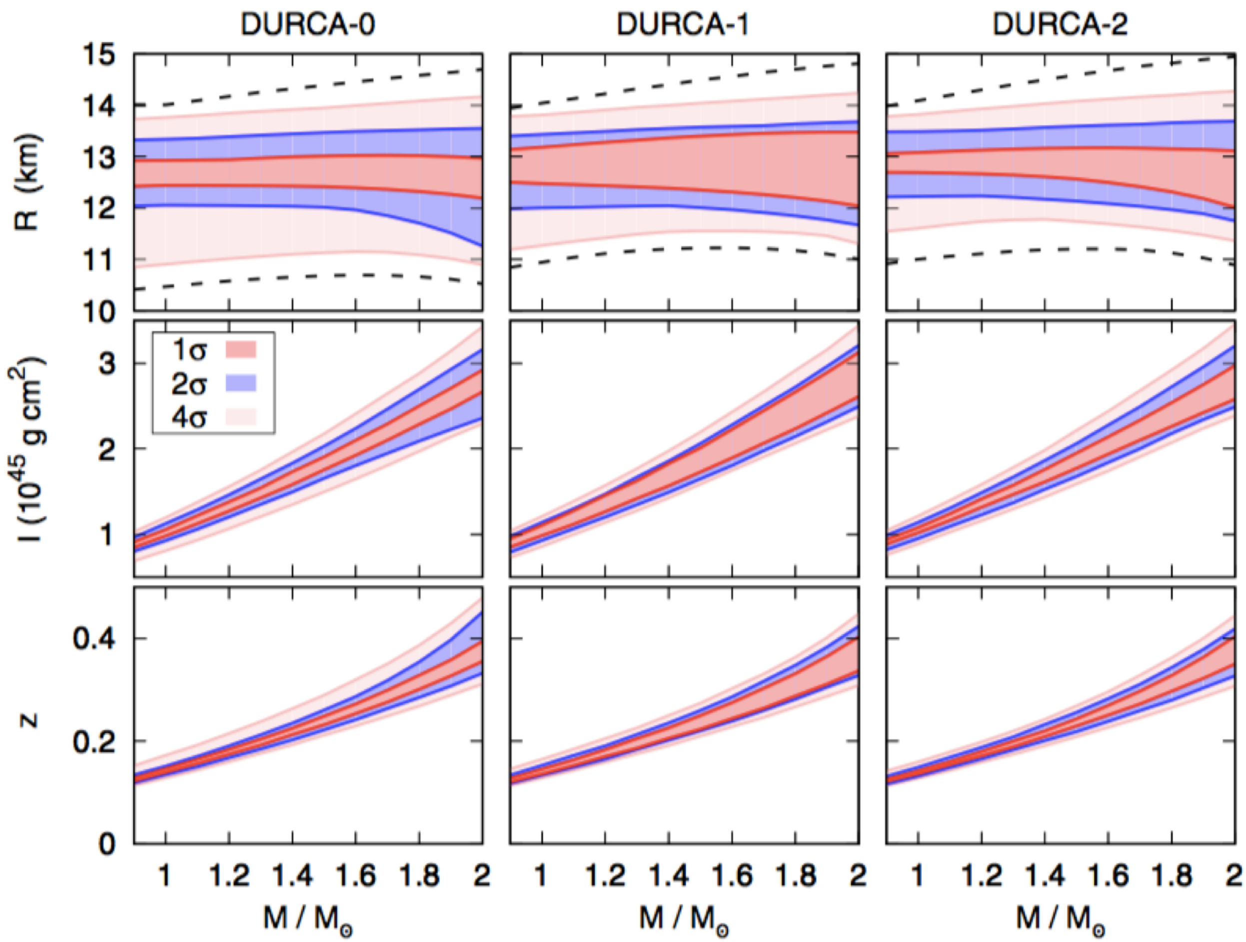

If composed exclusively of nucleons and leptons, our prediction is that neutron stars have a radius of 12.7 ± 0.4 km for masses between 1 and $2M_\odot$

J. Margueron, R. Hoffmann Casali, F. Gulminelli - Phys. Rev. C 97, 025806 (2018)

Predictions for neutron stars properties

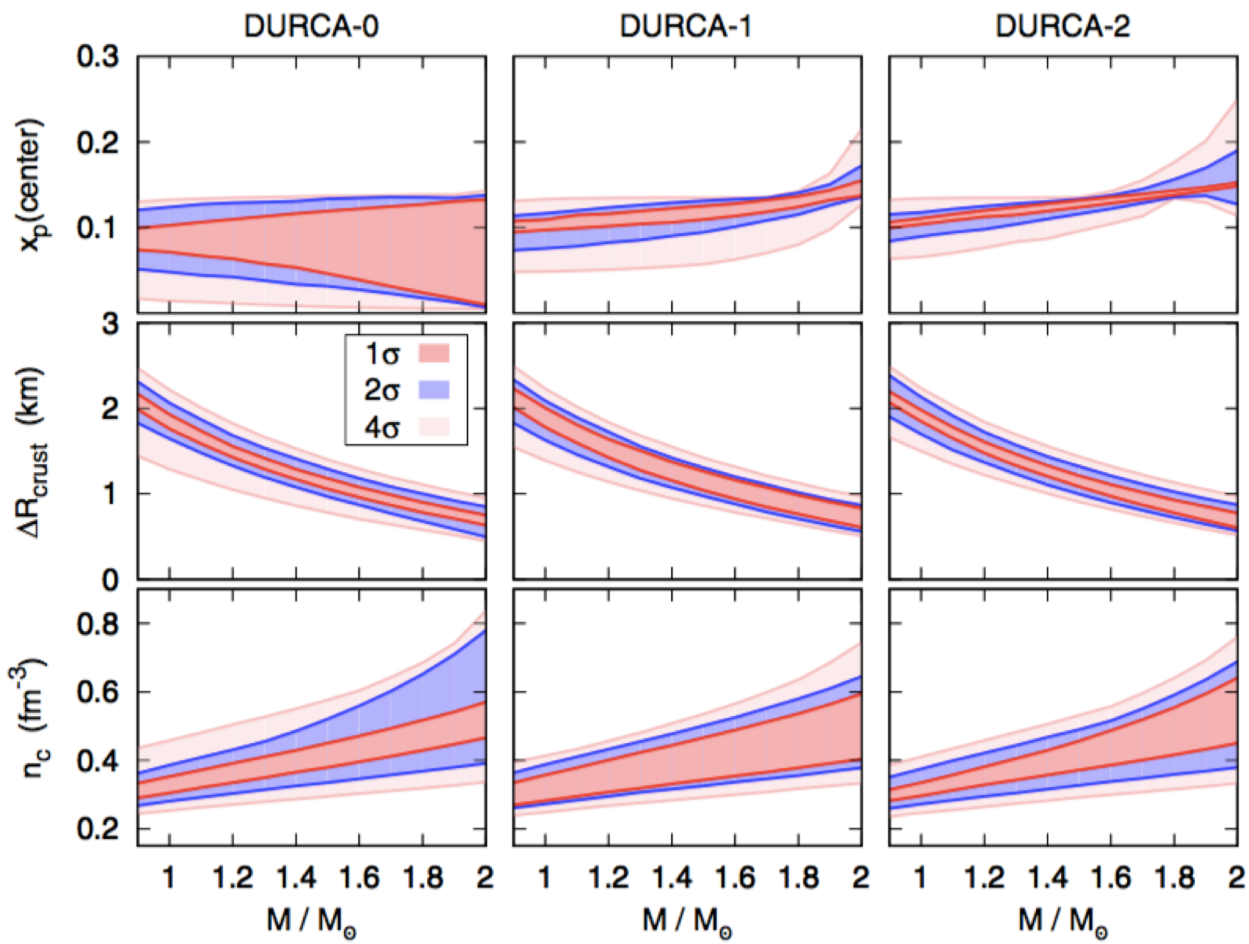

If composed exclusively of nucleons and leptons, our prediction is that neutron stars have a radius of 12.7 ± 0.4 km for masses between 1 and 2M$_\odot$

J. Margueron, R. Hoffmann Casali, F. Gulminelli - Phys. Rev. C 97, 025806 (2018)

GW170817
and
Tidal deformability

Hulse-Taylor pulsar – binary system

PSR B1913+16 (now J1915+1606)

Nobel Prize for Hulse and Taylor (1993)

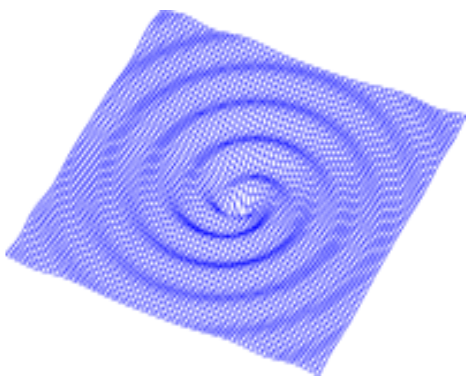

Excellent confirmation of Einstein theory of GW emission by observation of period decay

Anatomy of the GW signal

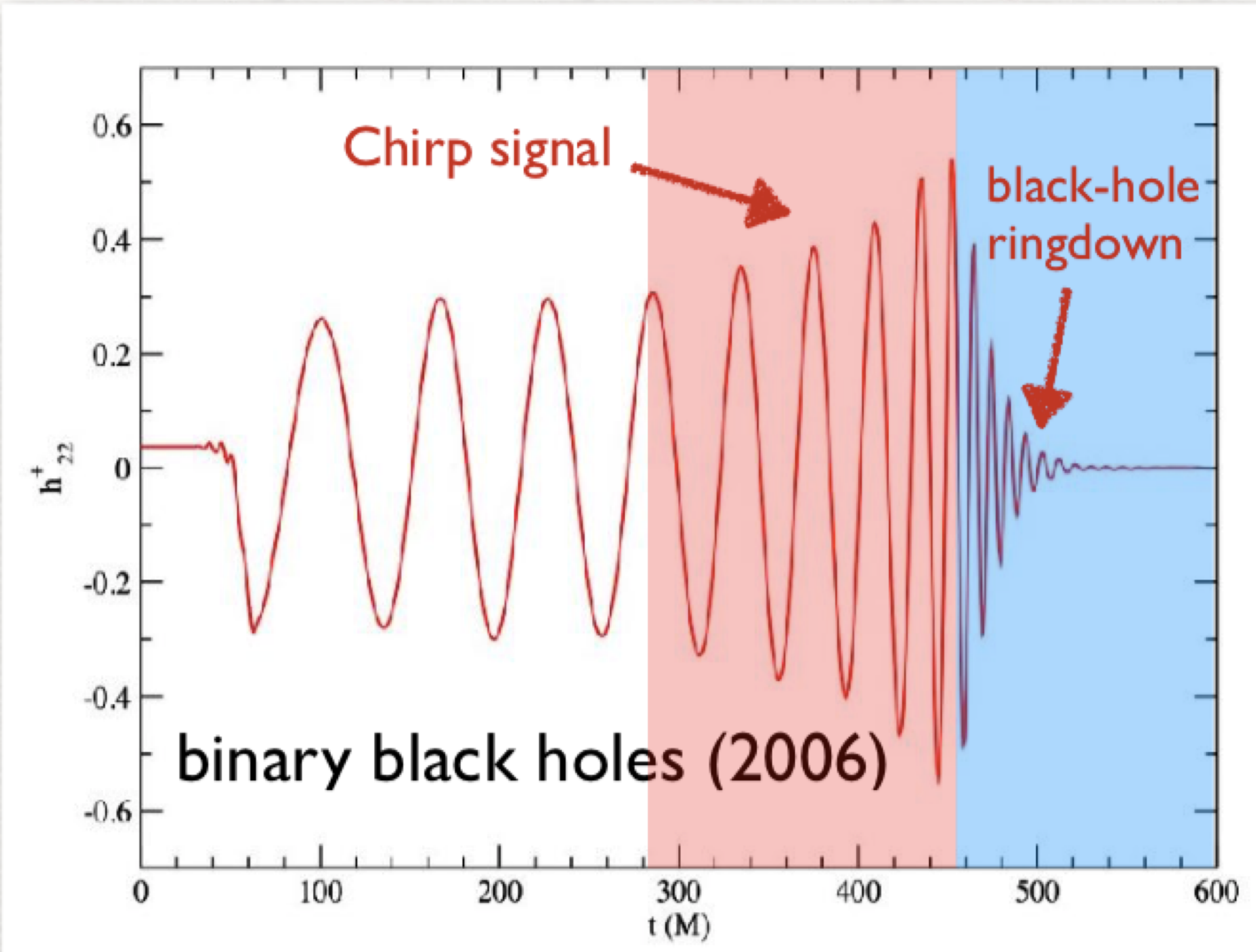

Anatomy of the GW signal

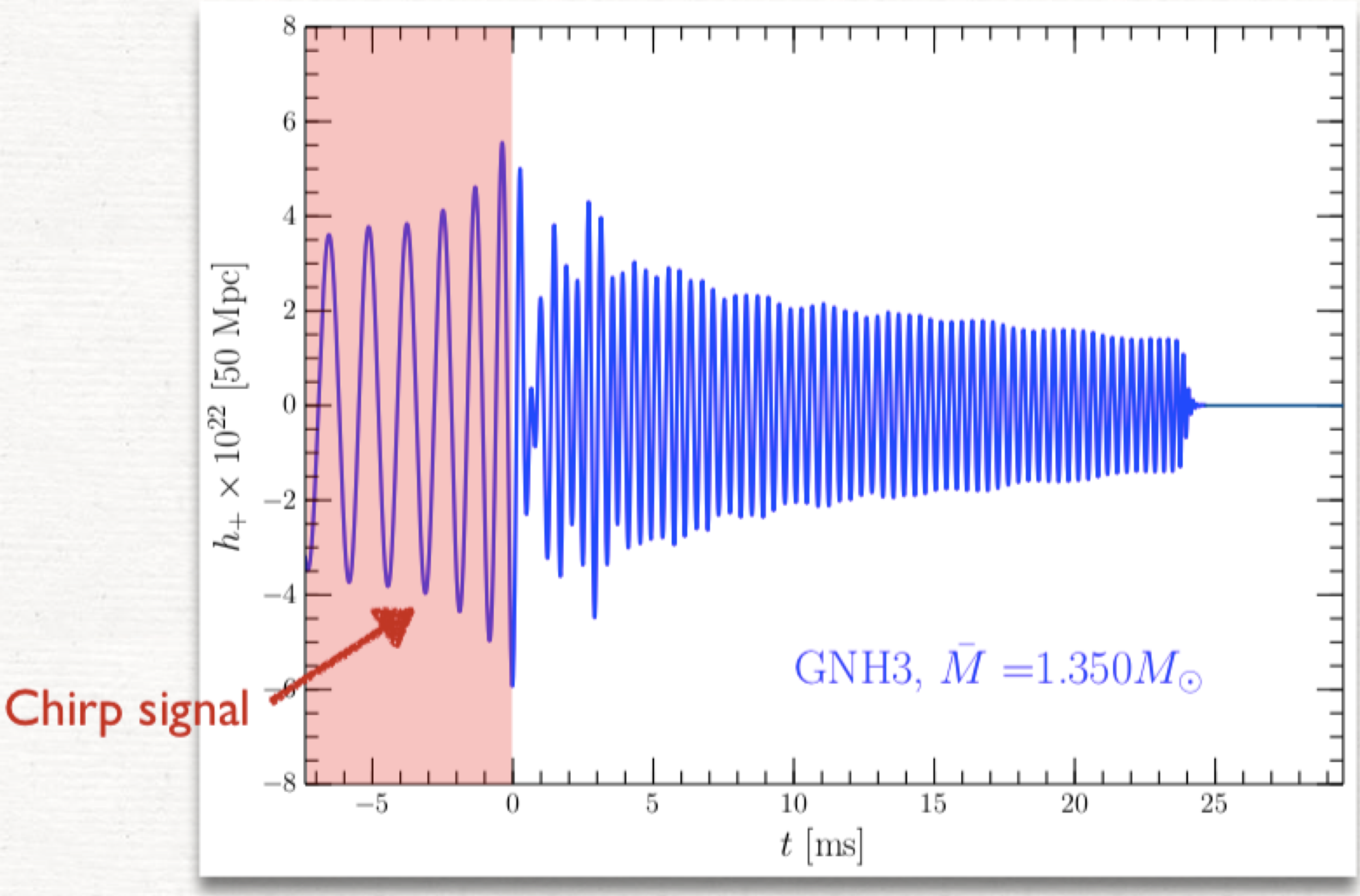

Direct measurement of gravitational waves – merging of two massive black holes (2015)

First detection of gravitational waves September 14, 2015 at 5:51 a.m. EDT (LIGO Collaboration)

Source at 410(18) Mpc [z=0.09(4)]

Initial black hole masses:
36(5) Mo and 29(4) Mo

Final black hole mass:
62(4) Mo

Energy release in gravitational waves
3.0(5) Mo c^2

Phys. Rev. Lett. 116, 061102 (2016)

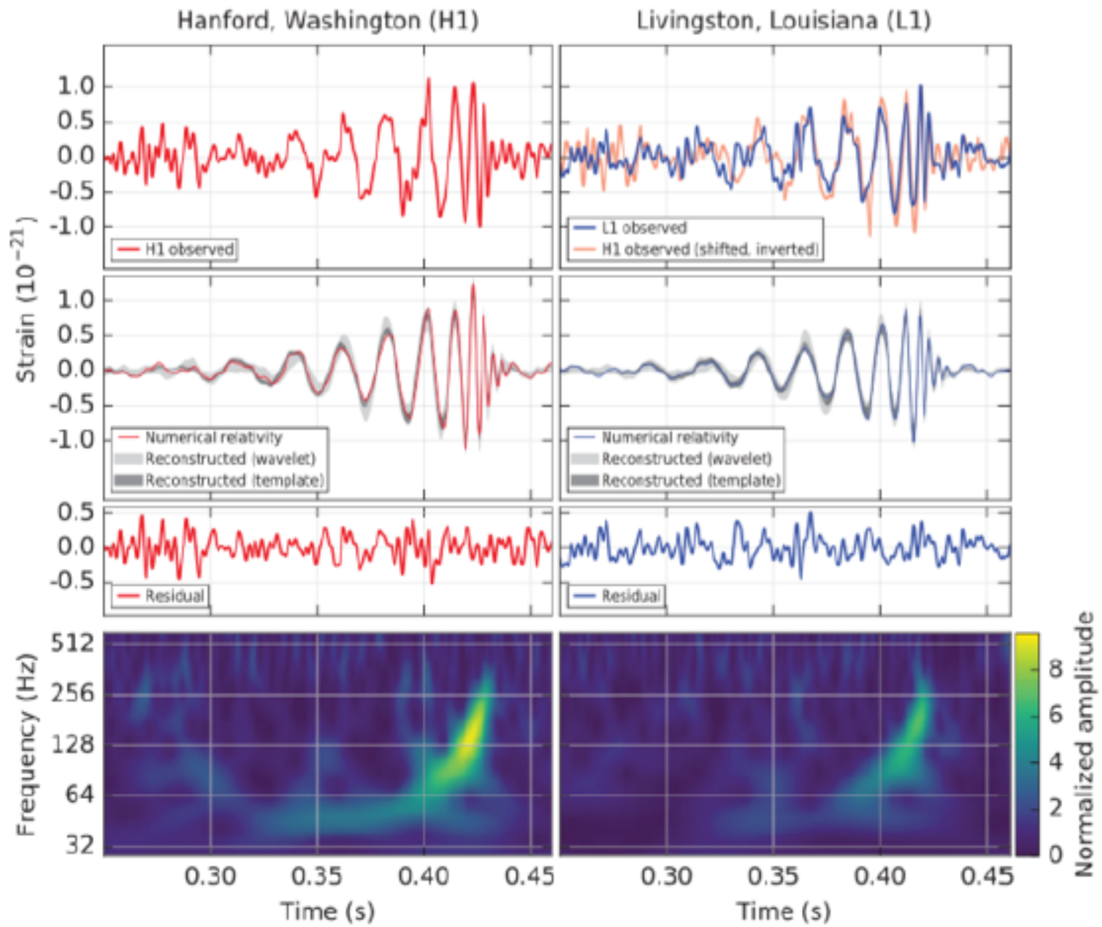

Nobel Prize Physics 2017 !! Rainer Weiss, Barry C. Barish, Kip Thorne

Ultimate goal: neutron star merger !

Simulated NS-NS merger events *)
--> Sensitivity to the NS equation of state!

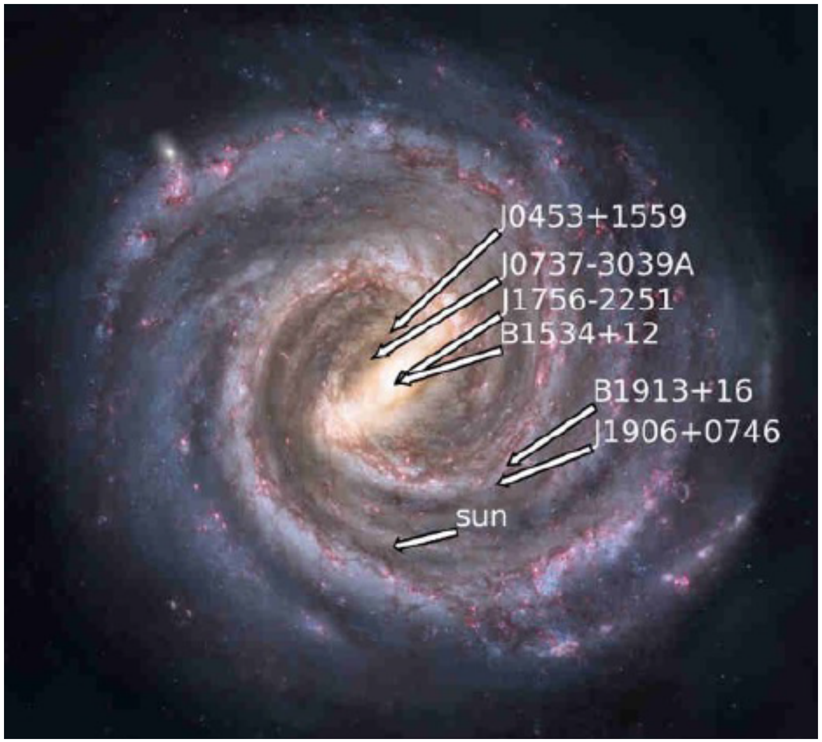

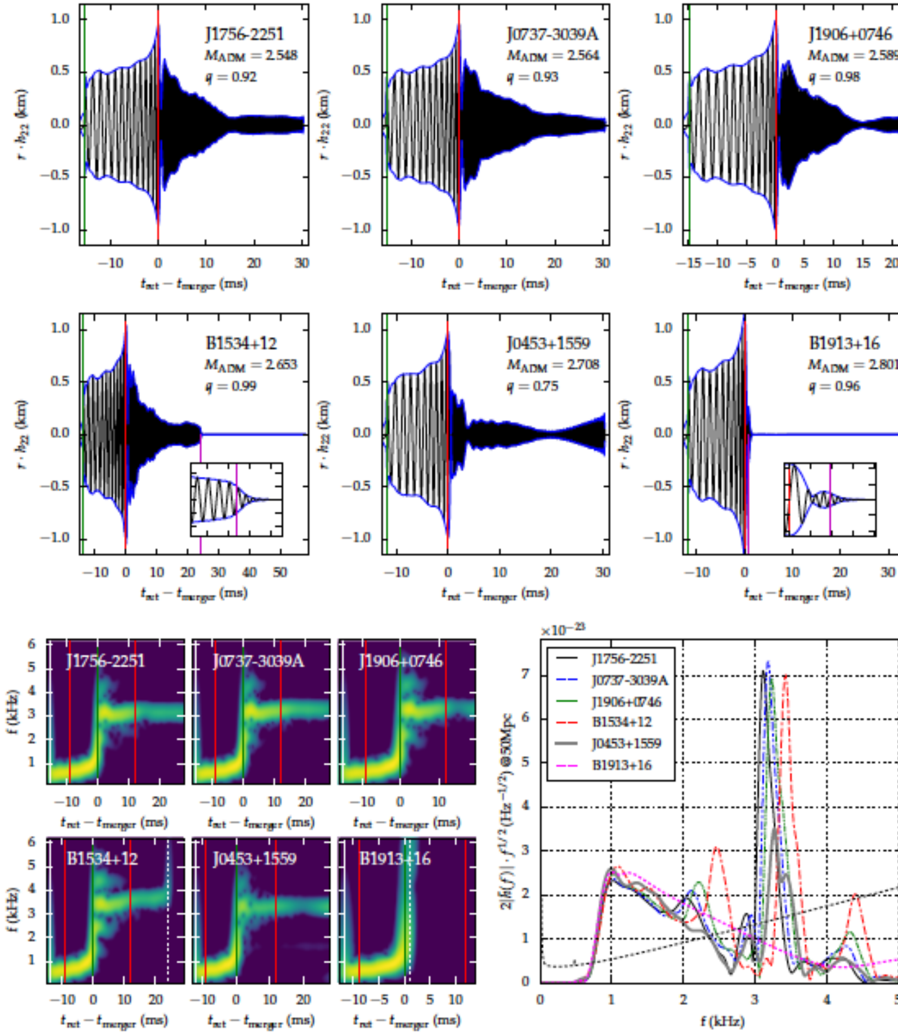

Expected rate ~ 0.2 – 200 events/year for
LIGO/Virgo Collaboration in 2016 - 2019

*) A. Feo, R. DePietri & F. Maione, Class. Quant. Grav. 34 (2017) 034001

Discovery: neutron star merger !

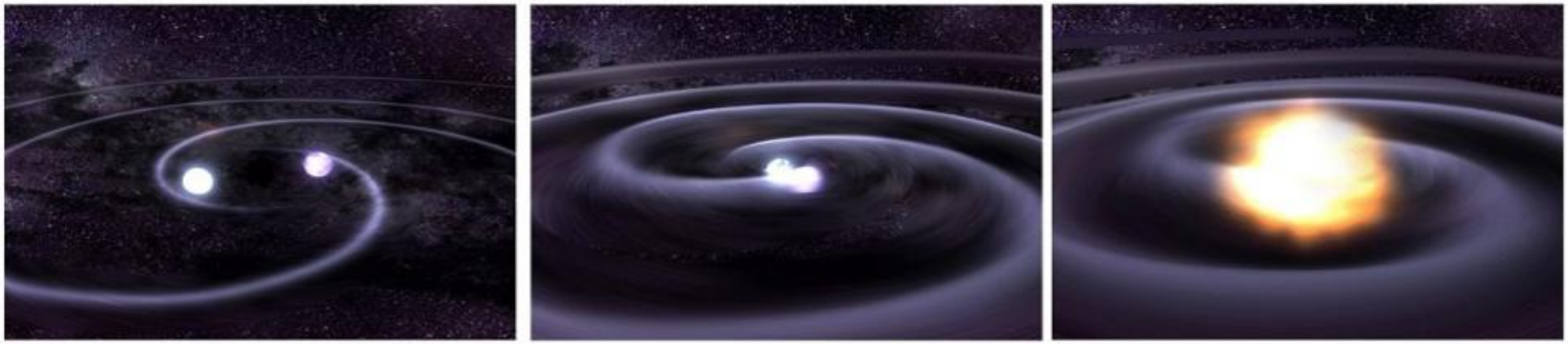

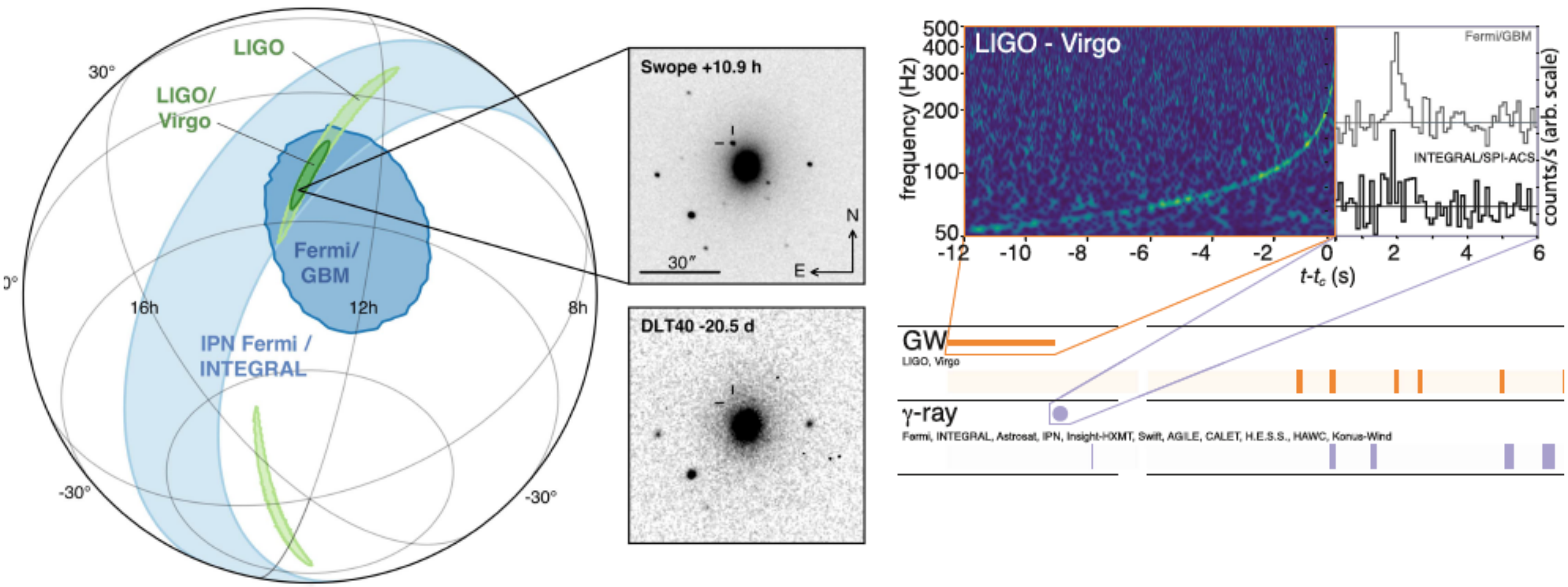

*) B.P. Abbott et al. [LIGO/Virgo Collab.], PRL 119, 161101 (2017); ApJLett 848, L12 (2017)

NS-NS merger !

GW170817A , announced 16.10.2017 → **Multi-Messenger Astrophysics !!**

	Low-spin prior ($\chi \leq 0.05$)	High-spin prior ($\chi \leq 0.89$)
Binary inclination θ_{JN}	146^{+25}_{-27} deg	152^{+21}_{-27} deg
Binary inclination θ_{JN} using EM distance constraint [108]	151^{+15}_{-11} deg	153^{+15}_{-11} deg
Detector-frame chirp mass $\mathcal{M}^{\rm det}$	$1.1975^{+0.0001}_{-0.0001}$ $M_\odot$	$1.1976^{+0.0004}_{-0.0002}$ $M_\odot$
Chirp mass $\mathcal{M}$	$1.186^{+0.001}_{-0.001}$ $M_\odot$	$1.186^{+0.001}_{-0.001}$ $M_\odot$
Primary mass m_1	$(1.36, 1.60)$ $M_\odot$	$(1.36, 1.89)$ $M_\odot$
Secondary mass m_2	$(1.16, 1.36)$ $M_\odot$	$(1.00, 1.36)$ $M_\odot$
Total mass m	$2.73^{+0.04}_{-0.01}$ $M_\odot$	$2.77^{+0.22}_{-0.05}$ $M_\odot$
Mass ratio q	(0.73, 1.00)	(0.53, 1.00)
Effective spin $\chi_{\rm eff}$	$0.00^{+0.02}_{-0.01}$	$0.02^{+0.08}_{-0.02}$
Primary dimensionless spin χ_1	(0.00, 0.04)	(0.00, 0.50)
Secondary dimensionless spin χ_2	(0.00, 0.04)	(0.00, 0.61)
Tidal deformability $\tilde{\Lambda}$ with flat prior	300^{+500}_{-190}(symmetric)/300^{+420}_{-230}(HPD)	(0, 630)

M<2.17 M_sun (arxiv:1710.05938)

B.P. Abbott et al. [LIGO/Virgo Collab.], PRL 119, 161101 (2017); Phys. Rev. X 9, 011001 (2019)

Implications from GW170817

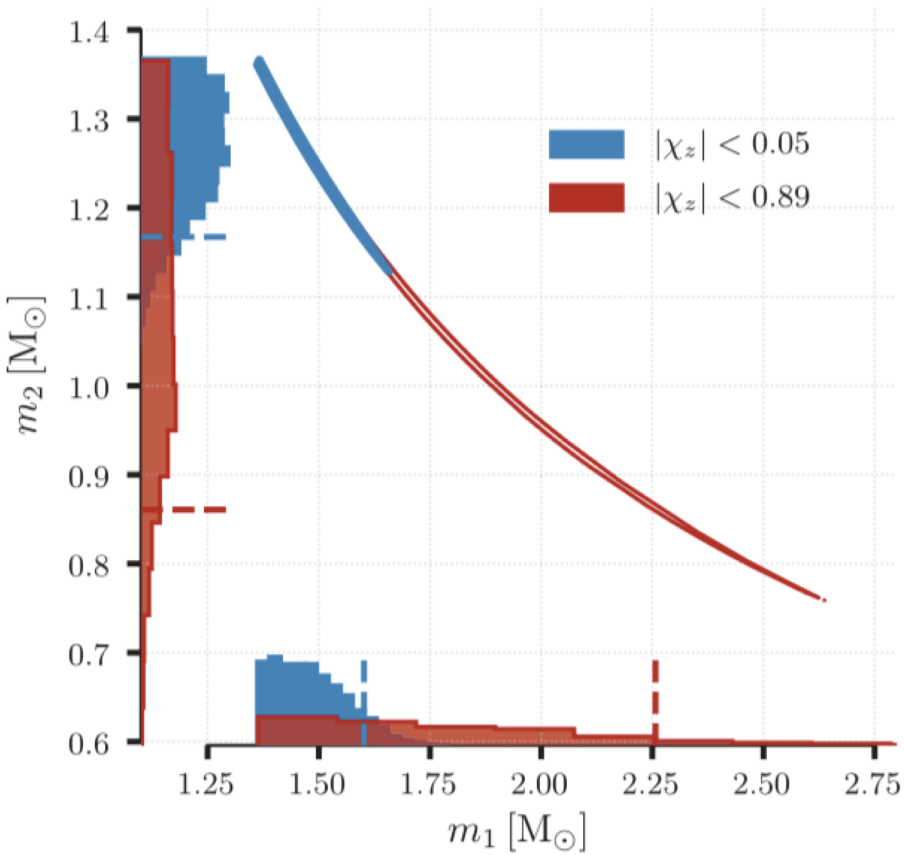

GW170817: Observation of Gravitational Waves from a Binary Neutron Star Inspiral
B. P. Abbott et al. arXiv:1712.00451

What can we learn from the inspiral II

- Waveforms incl. finite-size effects are described by tidal deformability (how a star reacts on an external tidal field)
- Offer possibility to constrain EoS because tidal deformability depends on EoS

$$\Lambda \equiv \frac{2}{3} k_2 \left(\frac{R}{M} \right)^5$$

- Corresponding to ~10 % error in radius R for nearby events (<100Mpc) (e.g. Read et al. 2013)
- Note: faithful templates to be constructed

R/M compactness (EoS dependent)

k_2 tidal love number (EoS dependent)

Computing the love number/tidal deformability

Extension of a standard TOV solver (i.e. numerically an integration of coupled ODEs):

Ansatz for the metric including a l=2 perturbation

$$
\begin{aligned}
ds^2 &= -e^{2\Phi(r)}\left[1+H(r)Y_{20}(\theta,\varphi)\right]dt^2 \\
&\quad +e^{2\Lambda(r)}\left[1-H(r)Y_{20}(\theta,\varphi)\right]dr^2 \\
&\quad +r^2\left[1-K(r)Y_{20}(\theta,\varphi)\right]\left(d\theta^2+\sin^2\theta d\varphi^2\right)
\end{aligned}
$$

Following Hinderer et al. 2010

Integrate standard TOV system:

$$
\begin{aligned}
e^{2\Lambda} &= \left(1-\frac{2m_r}{r}\right)^{-1}, \\
\frac{d\Phi}{dr} &= -\frac{1}{\epsilon+p}\frac{dp}{dr}, \\
\frac{dp}{dr} &= -(\epsilon+p)\frac{m_r+4\pi r^3 p}{r(r-2m_r)}, \\
\frac{dm_r}{dr} &= 4\pi r^2\epsilon.
\end{aligned}
$$

EoS to be provided ε(p)

And additional eqs. for perturbations:

$$
\begin{aligned}
\frac{dH}{dr} &= \beta \qquad (11)\\
\frac{d\beta}{dr} &= 2\left(1-2\frac{m_r}{r}\right)^{-1} H\left\{-2\pi\left[5\epsilon+9p+f(\epsilon+p)\right]\right. \\
&\quad \left.+\frac{3}{r^2}+2\left(1-2\frac{m_r}{r}\right)^{-1}\left(\frac{m_r}{r^2}+4\pi rp\right)^2\right\} \\
&\quad +\frac{2\beta}{r}\left(1-2\frac{m_r}{r}\right)^{-1}\left\{-1+\frac{m_r}{r}+2\pi r^2(\epsilon-p)\right\}.
\end{aligned}
$$

(K(r) given by H(r))

Note: Although multidimensional problem – computation in 1D since absorbed in Y20

Love number

$$y = \frac{R\beta(R)}{H(R)}$$

$$\begin{aligned} k_2 \; = \; & \frac{8C^5}{5}(1-2C)^2[2+2C(y-1)-y] \\ & \times\Big\{2C[6-3y+3C(5y-8)] \\ & +4C^3[13-11y+C(3y-2)+2C^2(1+y)] \\ & +3(1-2C)^2[2-y+2C(y-1)]\ln(1-2C)\Big\}^{-1} \end{aligned}$$

where $C = M/R$ is the compactness of the star.

Implications from GW170817

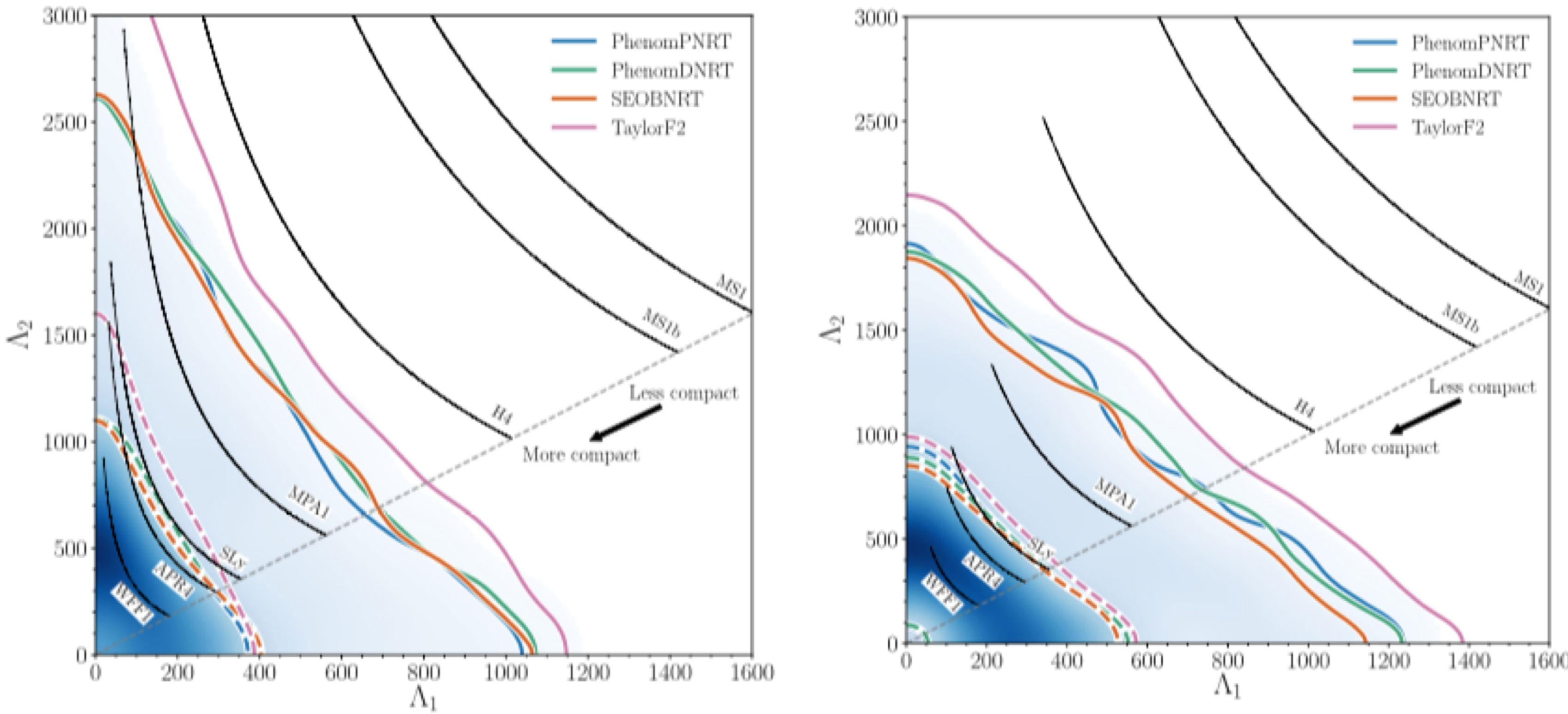

Properties of the Binary Star Merger GW170817
B. P. Abbott et al., Phys. Rev. X 9, 011001 (2019)

Symmetry energy effects

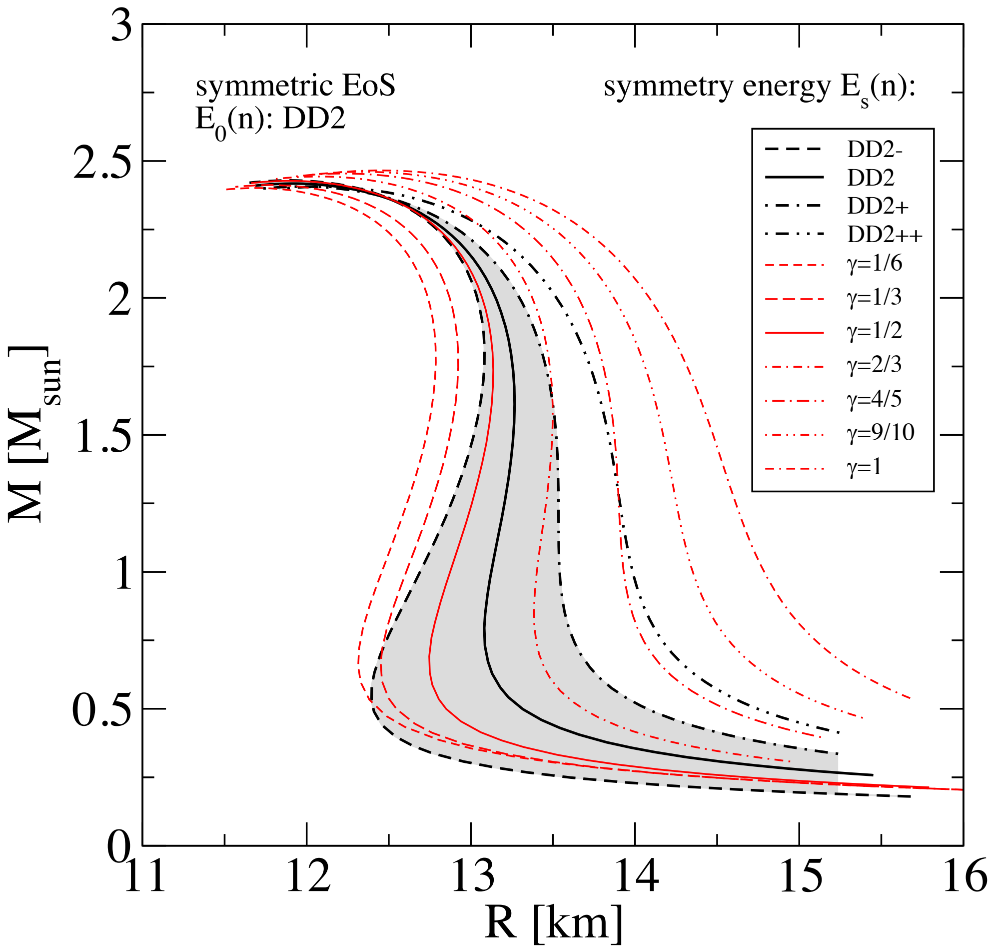

Implications from GW170817

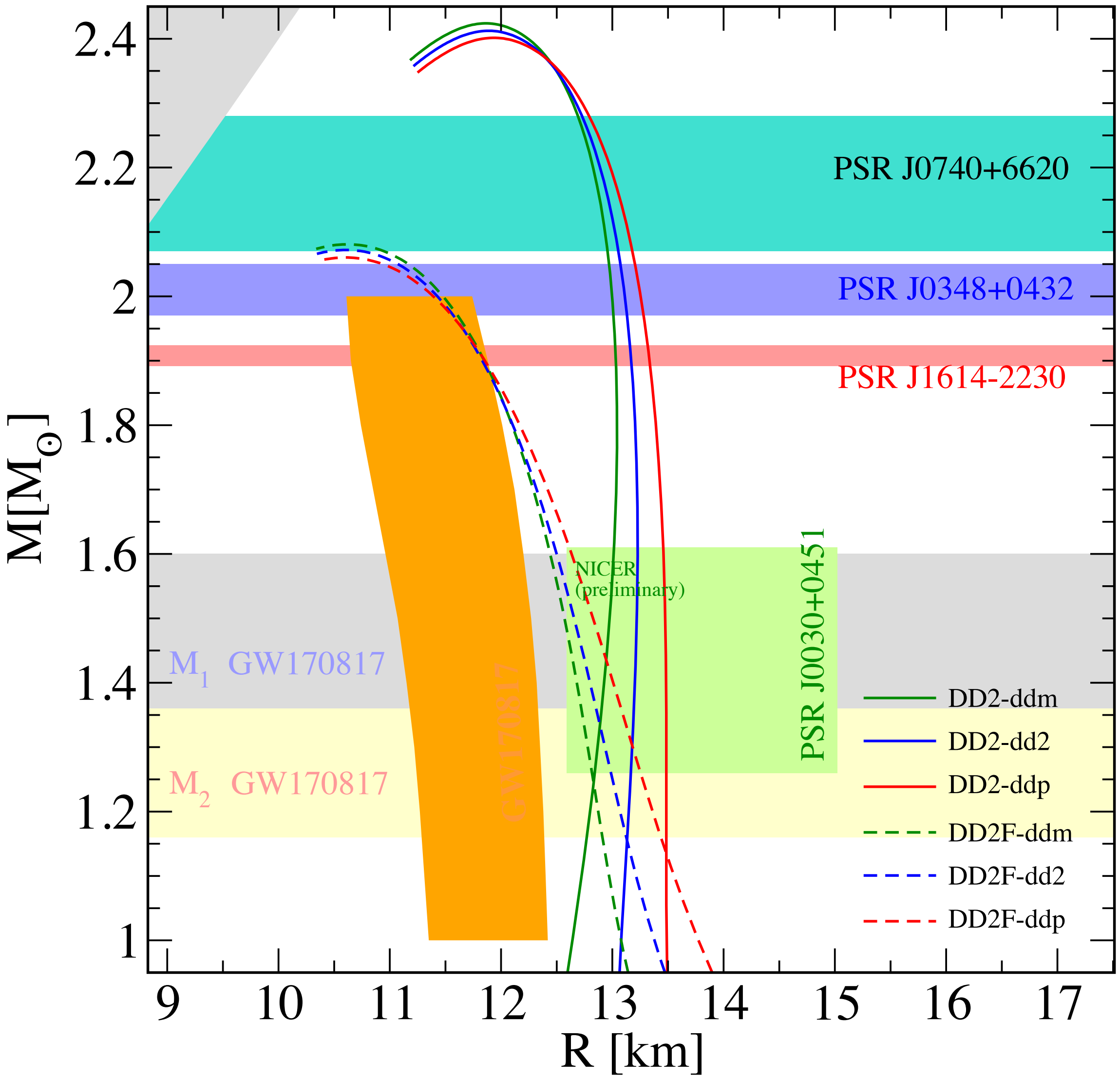

Implications from GW170817

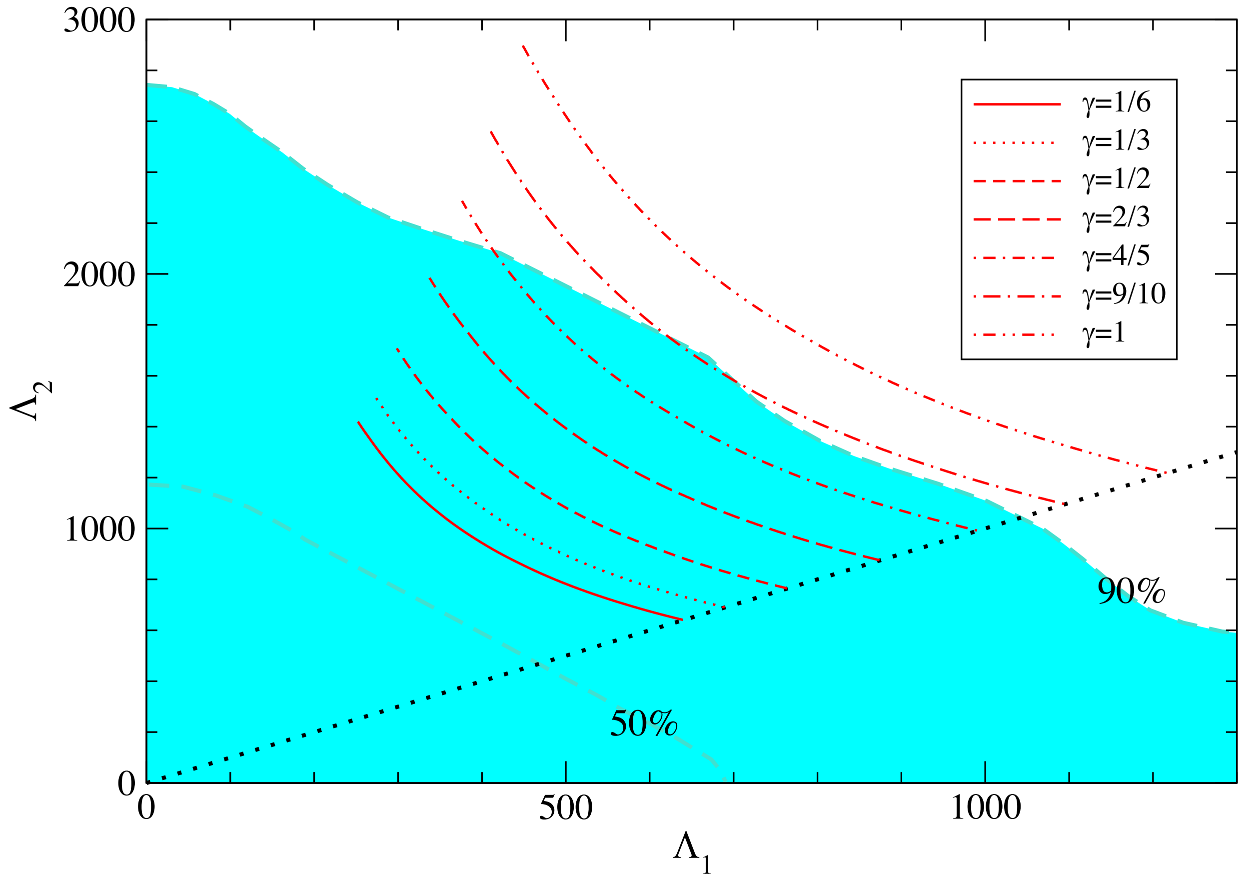

Implications from GW170817

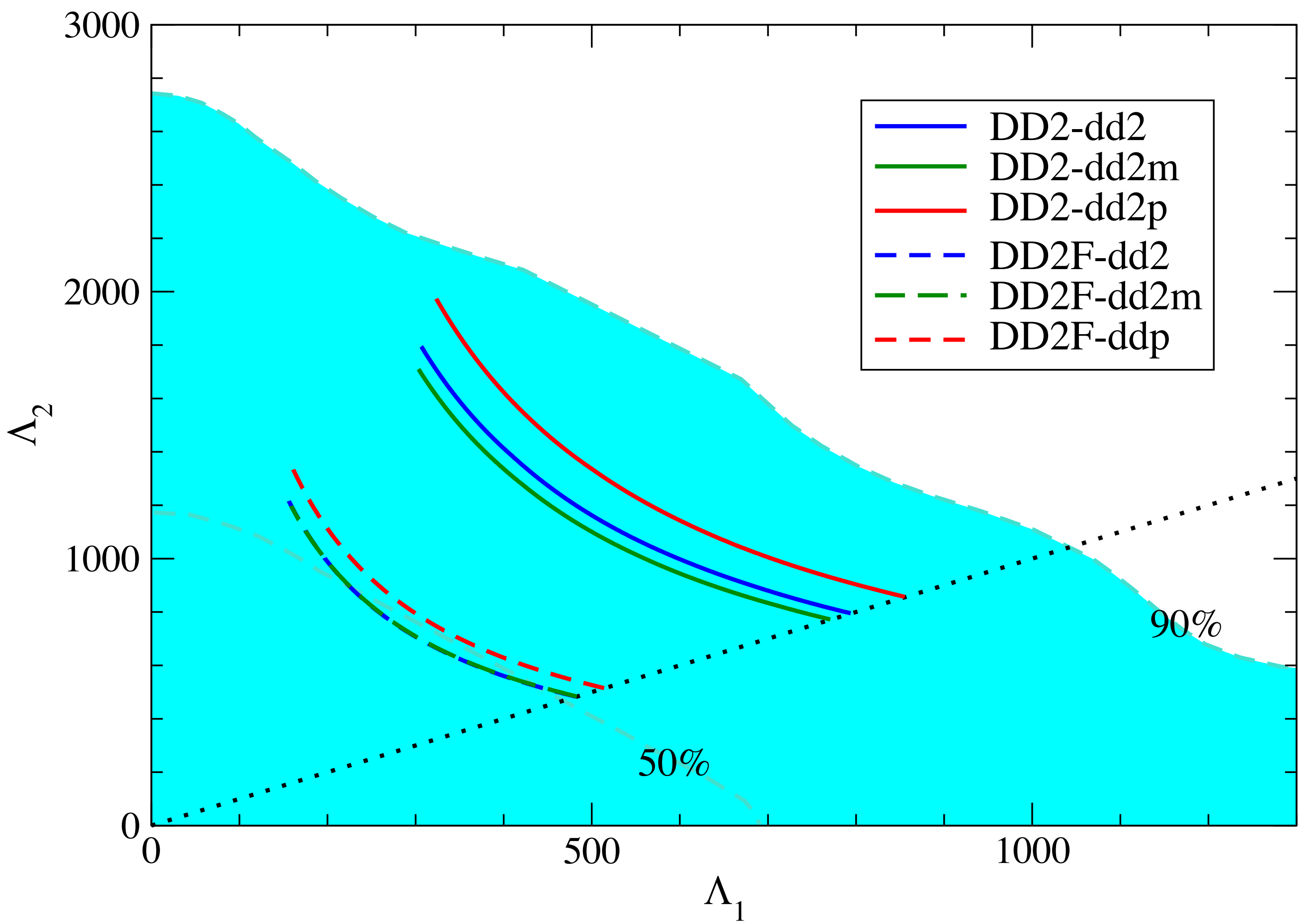

Critical Endpoint in QCD

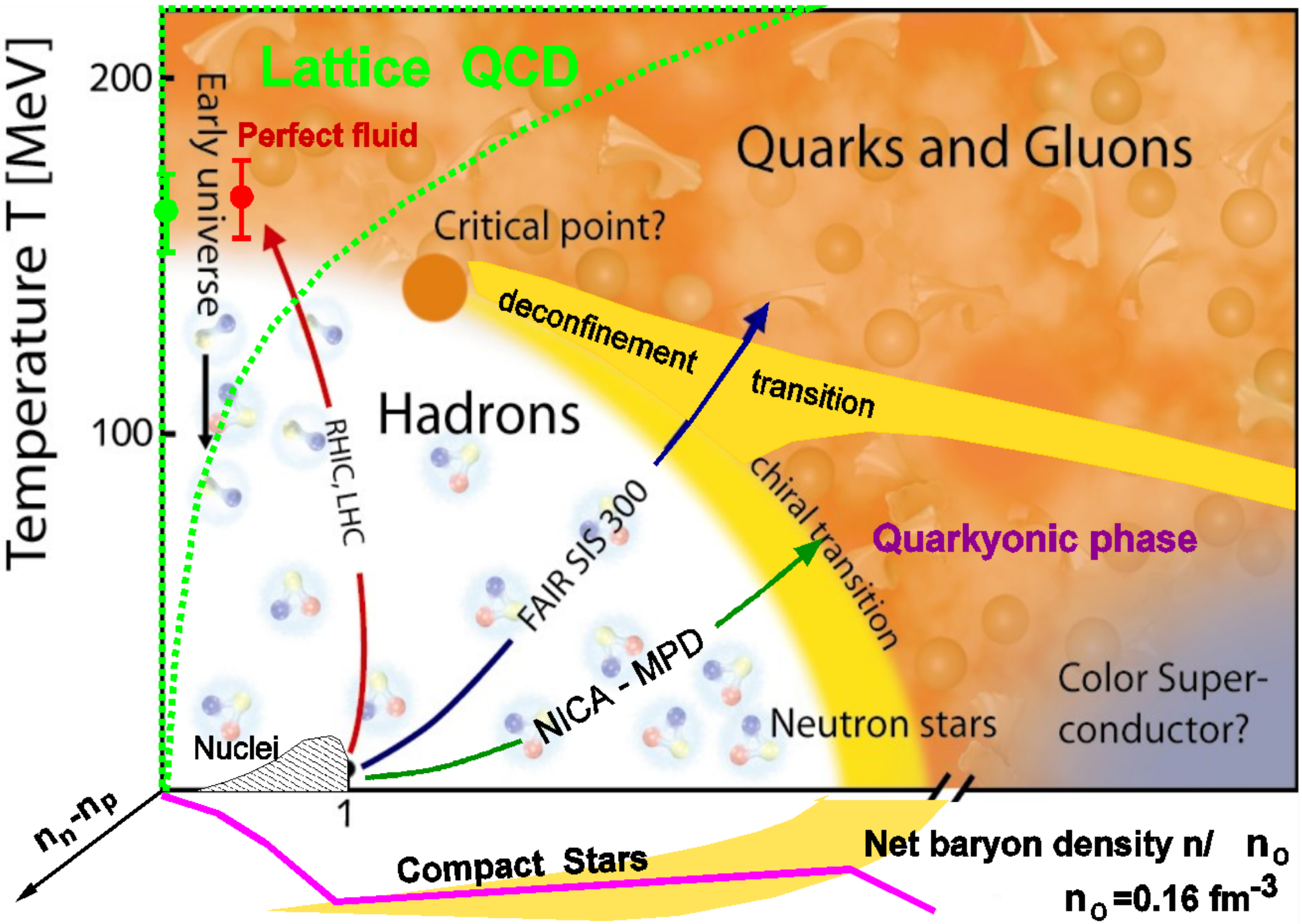

Critical Endpoint in QCD

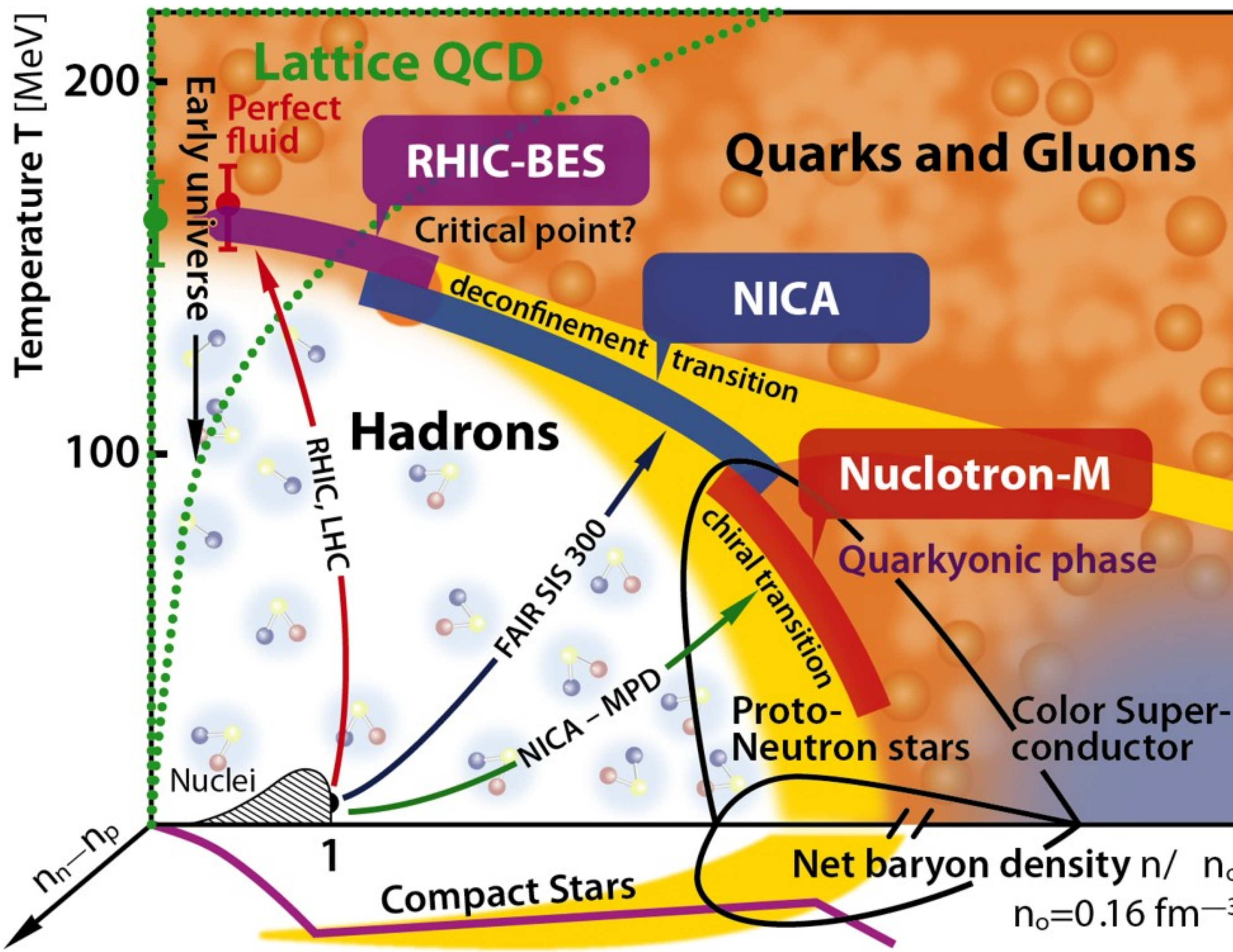

Piecewise polytrope EoS

Hebeler et al., ApJ 773, 11 (2013)

$$P_i(n) = \kappa_i n^{\Gamma_i}$$

$$i = 1 \;:\; n_1 \leq n \leq n_{12}$$
$$i = 2 \;:\; n_{12} \leq n \leq n_{23}$$
$$i = 3 \;:\; n \geq n_{23}\;,$$

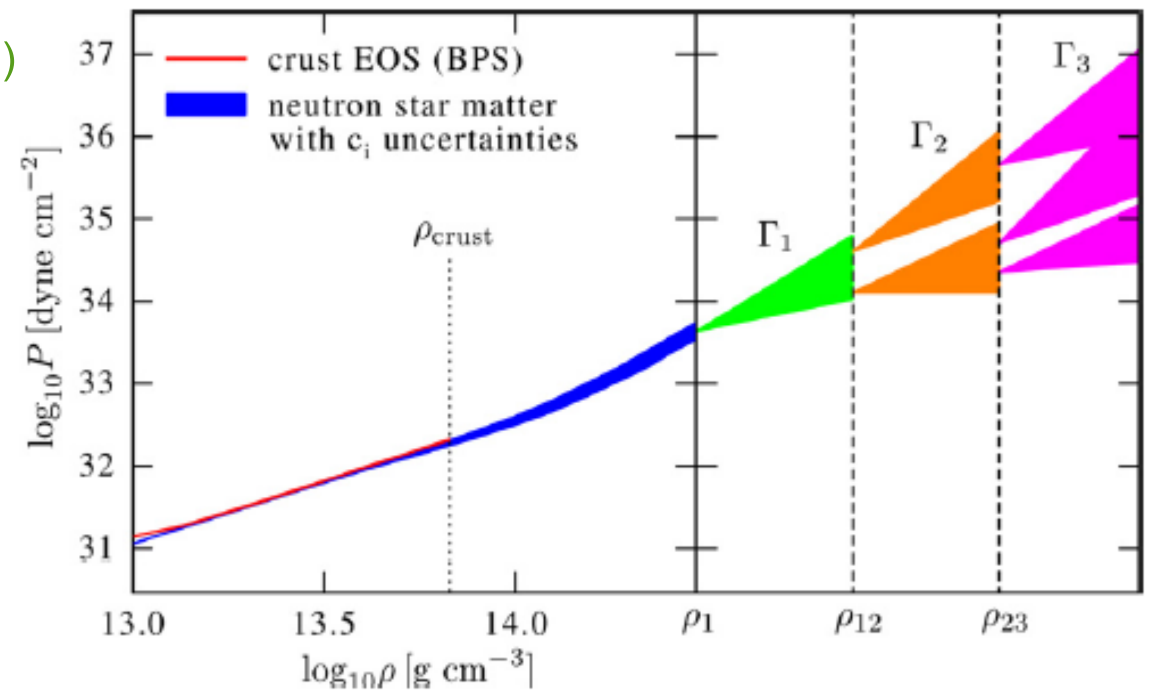

Here, 1st order PT in region 2:

$$\Gamma_2 = 0 \text{ and } P_2 = \kappa_2 = P_{\text{crit}}$$

$$P(n) = n^2 \frac{d(\varepsilon(n)/n)}{dn},$$
$$\varepsilon(n)/n = \int dn\, \frac{P(n)}{n^2} = \int dn\, \kappa n^{\Gamma-2} = \frac{\kappa\, n^{\Gamma-1}}{\Gamma-1} + C,$$
$$\mu(n) = \frac{P(n)+\varepsilon(n)}{n} = \frac{\kappa\,\Gamma}{\Gamma-1} n^{\Gamma-1} + m_0,$$

$$n(\mu) = \left[(\mu - m_0)\frac{\Gamma-1}{\kappa\Gamma}\right]^{1/(\Gamma-1)}$$
$$P(\mu) = \kappa\left[(\mu - m_0)\frac{\Gamma-1}{\kappa\Gamma}\right]^{\Gamma/(\Gamma-1)}$$

Maxwell construction:

$$P_1(\mu_{\text{crit}}) = P_3(\mu_{\text{crit}}) = P_{\text{crit}}$$
$$\mu_{\text{crit}} = \mu_1(n_{12}) = \mu_3(n_{23})$$

Seidov criterion for instability: $\frac{\Delta\varepsilon}{\varepsilon_{\text{crit}}} \geq \frac{1}{2} + \frac{3}{3}\frac{P_{\text{crit}}}{\varepsilon_{\text{crit}}}$

Compact Star Twins

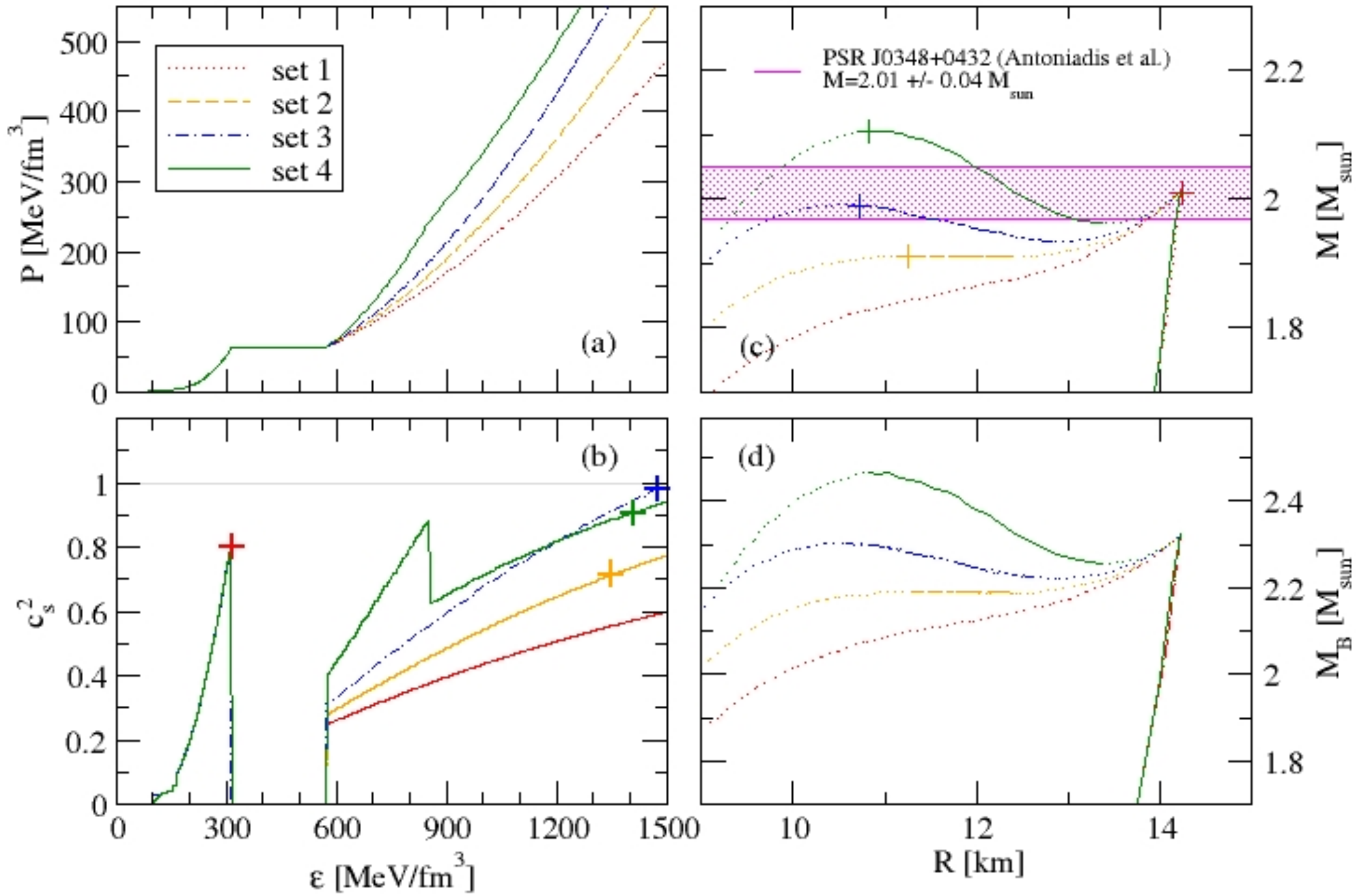

Alvarez-Castillo, Blaschke (2017)
High mass twins from multi-polytrope equations of state
arXiv: 1703.02681v2, Phys. Rev. C 96, 045809 (2017)

Energy bursts from deconfinement

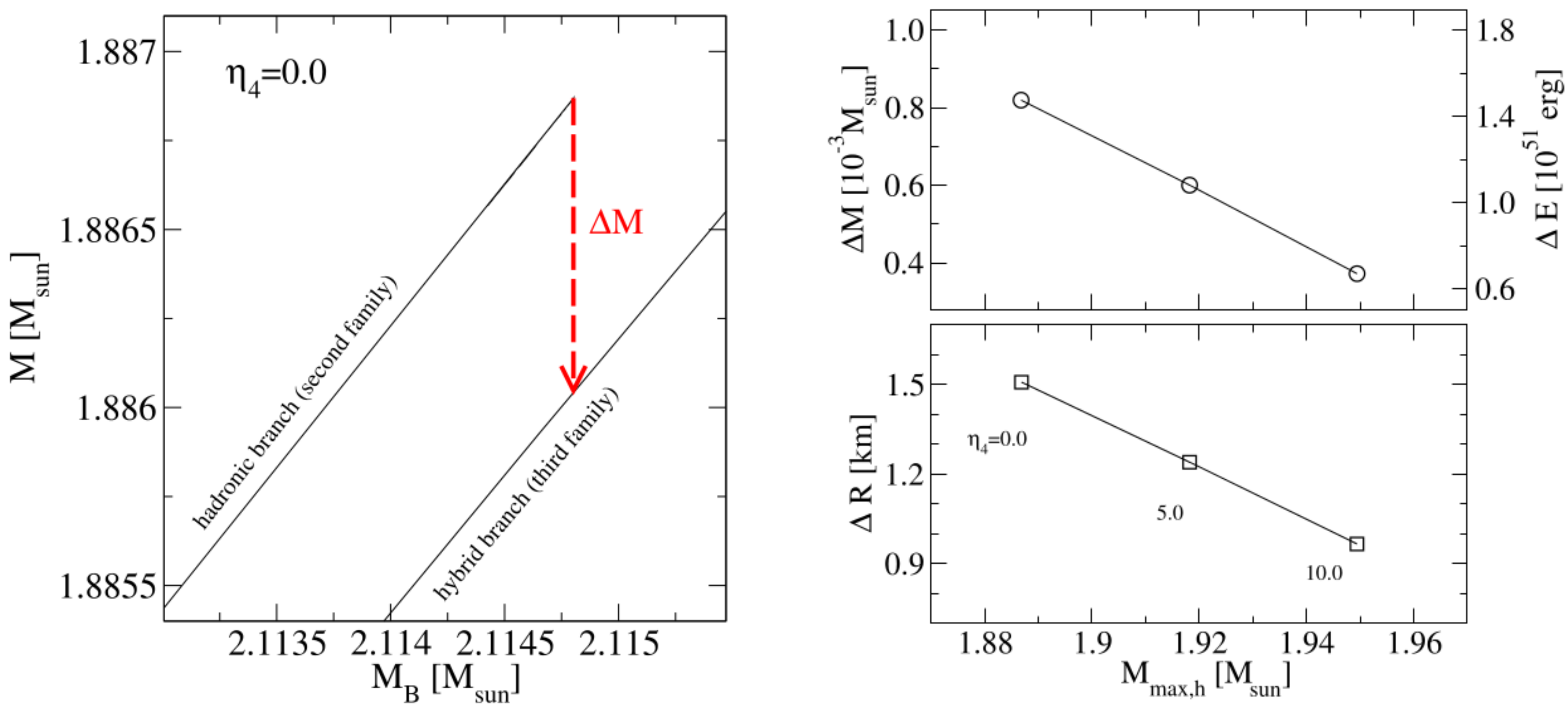

Alvarez-Castillo, Bejger, Blaschke, Haensel, Zdunik (2015), arXiv:1401.5380

Implications from GW170817

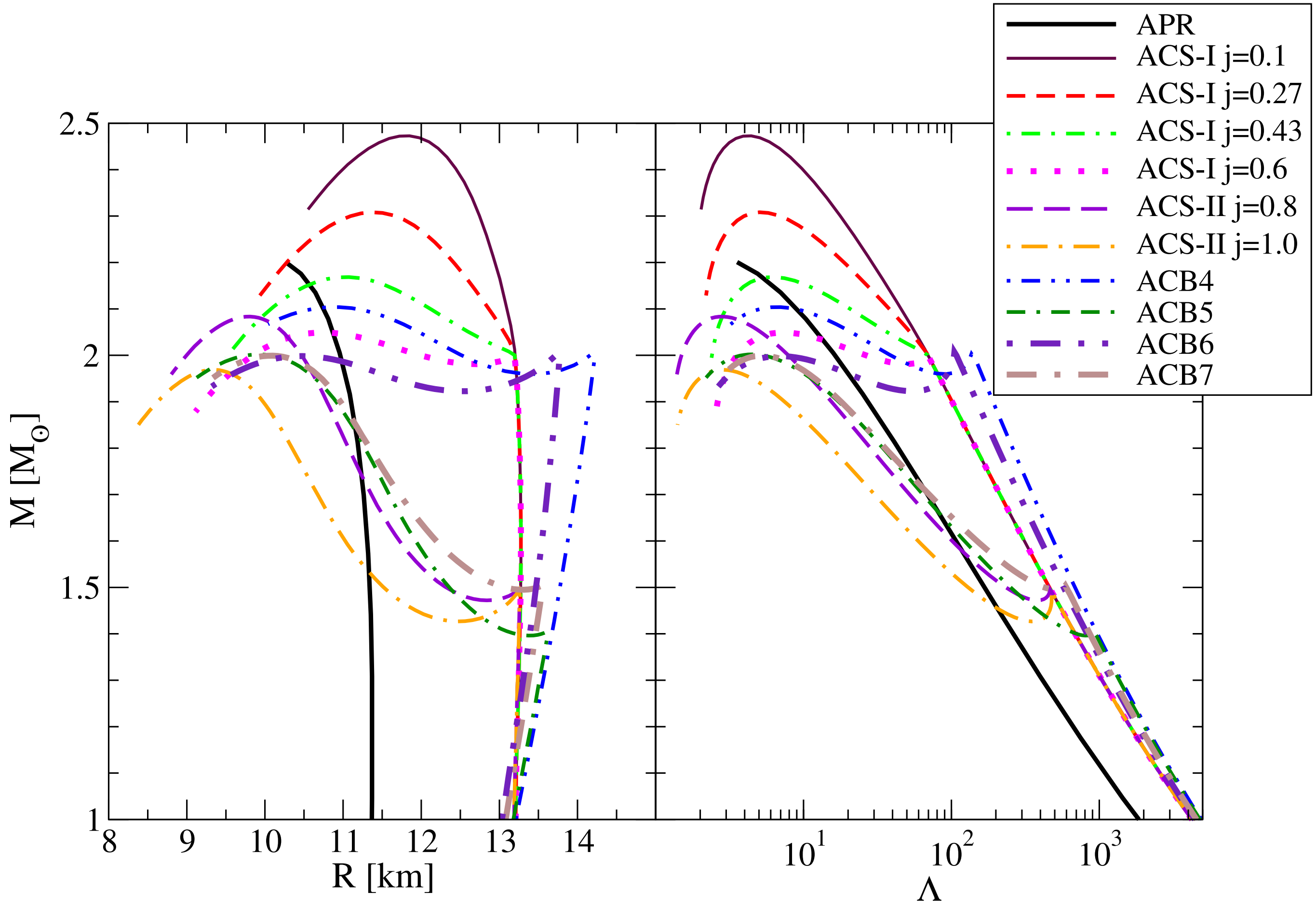

Vasileios Paschalidis, Kent Yagi, David Alvarez-Castillo, David B. Blaschke, Armen Sedrakian
Phys. Rev. D 97, 084038 (2018), arXiv:1712.00451

Implications from GW170817

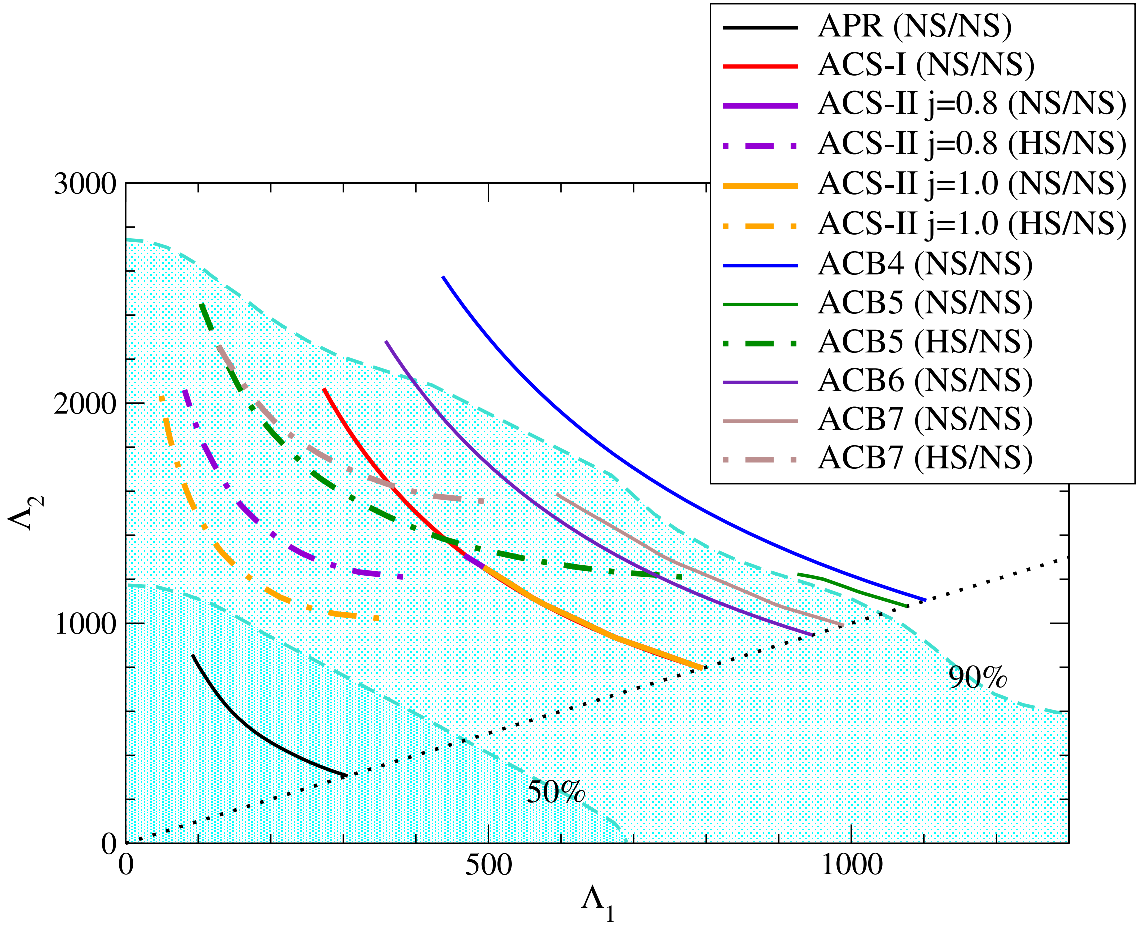

Vasileios Paschalidis, Kent Yagi, David Alvarez-Castillo,
David B. Blaschke, Armen Sedrakian
Phys. Rev. D 97, 084038 (2018), arXiv:1712.00451

Implications from GW170817 and I-Love-Q relations

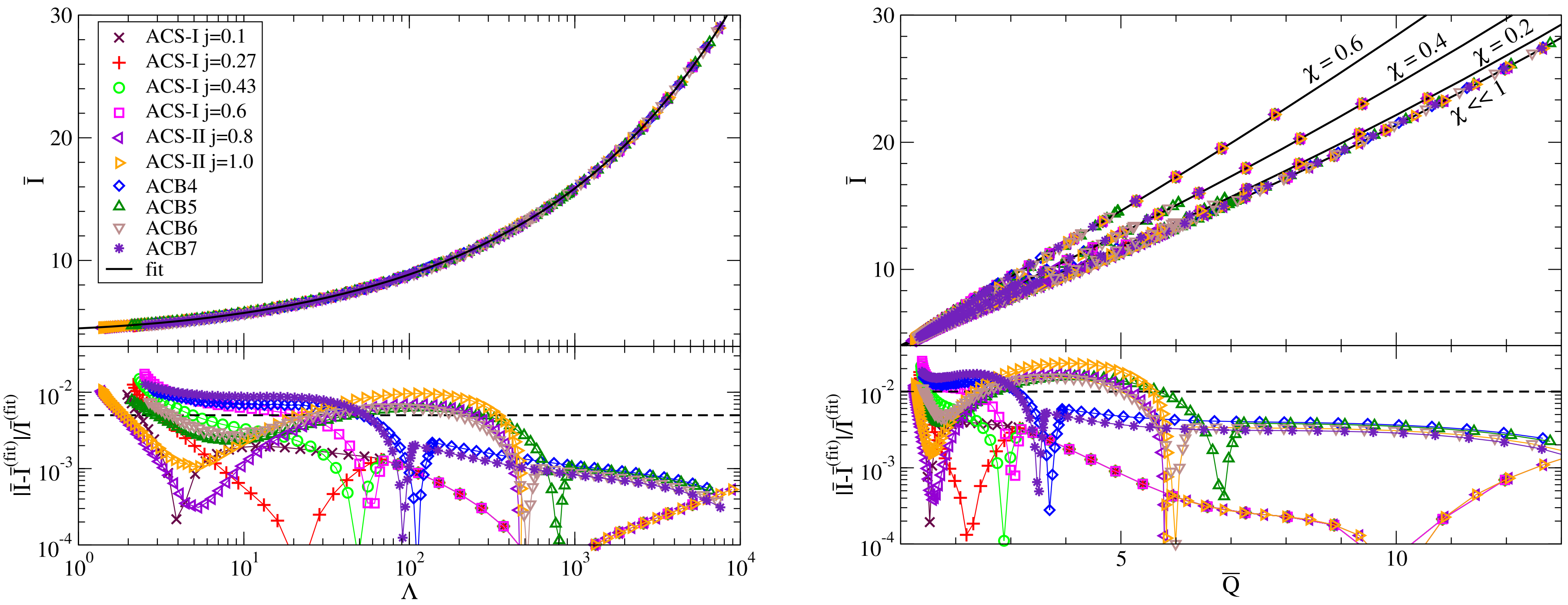

Vasileios Paschalidis, Kent Yagi, David Alvarez-Castillo,
David B. Blaschke, Armen Sedrakian
Phys. Rev. D 97, 084038 (2018), arXiv:1712.00451

Implications from GW170817
Nonlocal NJL

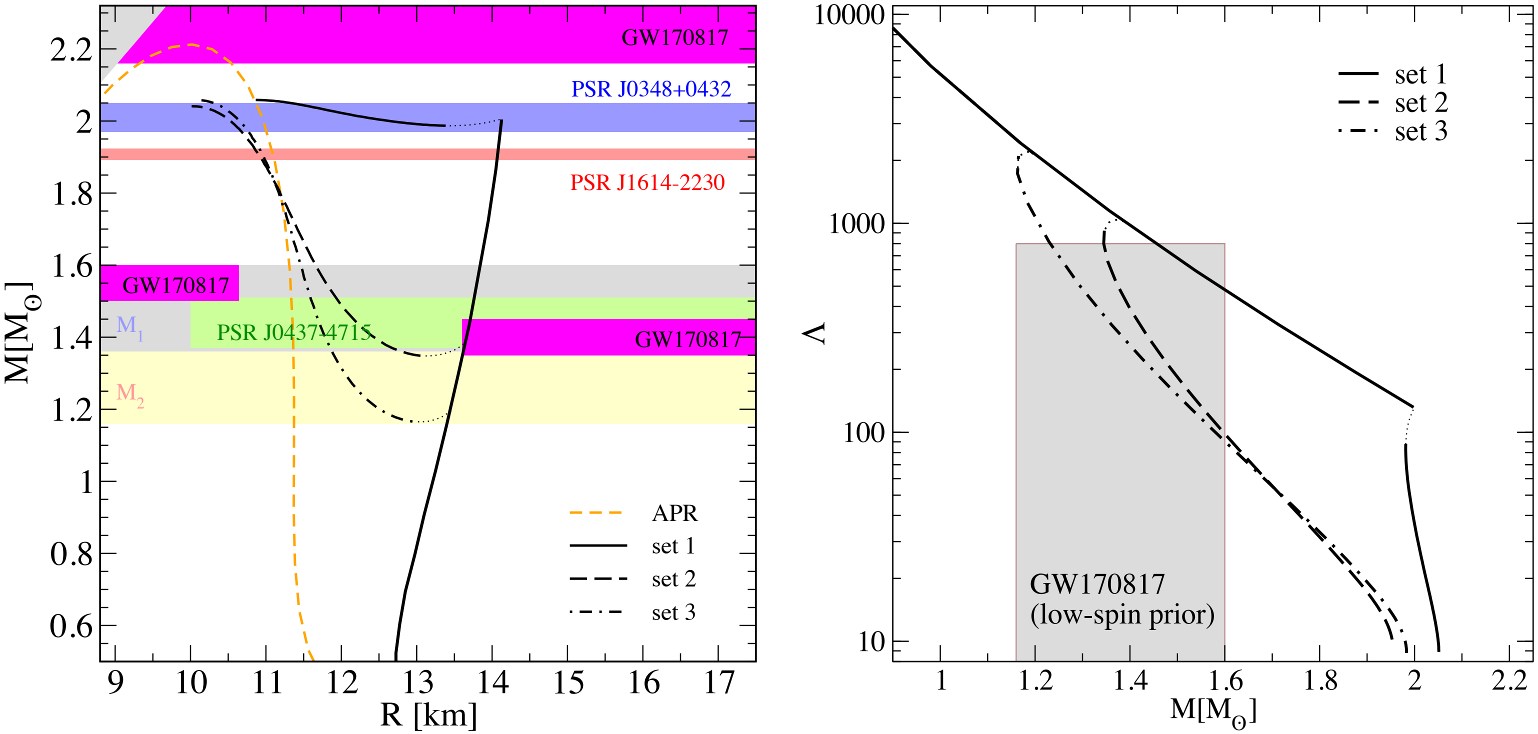

D. Alvarez-Castillo, D. Blaschke, G. Grunfeld, V. Pagura
Phys. Rev. D 99, 063010 (2019) - arXiv: 1805.04105

Moments of Inertia

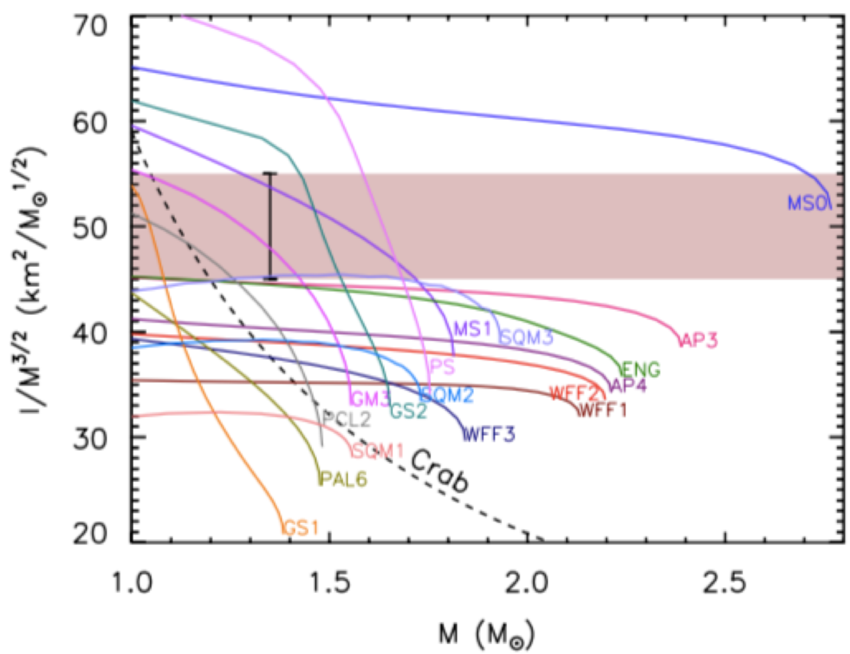

Fig. 9. The moment of inertia scaled by $M^{3/2}$ as a function of stellar mass M for EOSs described in [6]. The shaded band illustrates a $\pm 10\%$ error on a hypothetical $I/M^{3/2}$ measurement with centroid $50\,\text{km}^2\,\text{M}_\odot^{-1/2}$; the error bar shows the specific case in which the mass is $1.34\,\text{M}_\odot$ with essentially no error. The dashed curve labelled "Crab" is the lower limit derived by [123] for the Crab pulsar.

$$I \simeq \frac{J}{1 + 2GJ/R^3c^2}, \quad J = \frac{8\pi}{3}\int_0^R r^4\left(\rho + \frac{p}{c^2}\right)\Lambda dr, \quad \Lambda = \frac{1}{1 - 2Gm/rc^2}$$

MEASUREMENT OF SPIN PRECESION OF A PULSAR

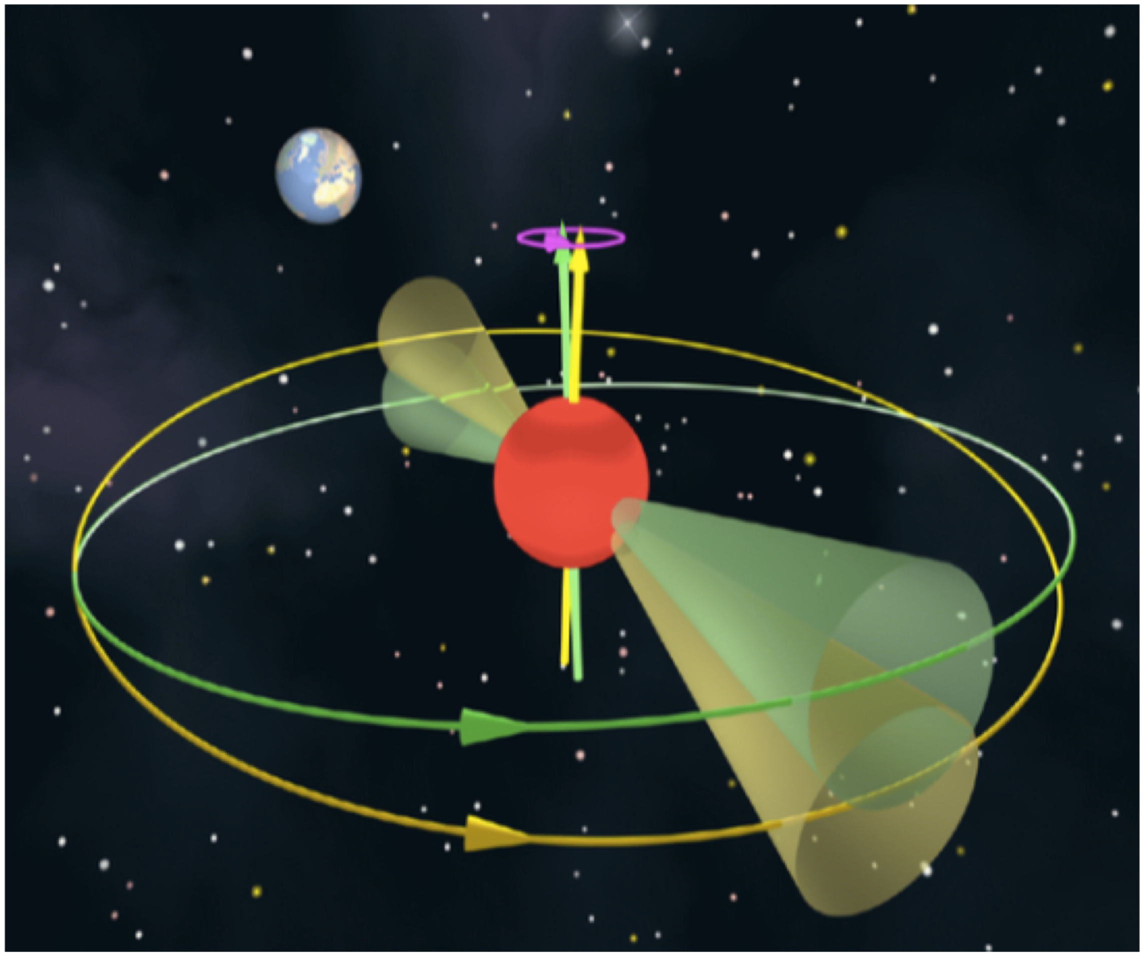

Perspectives for new Instruments?

THE FUTURE: SKA - SQUARE KILOMETER ARRAY

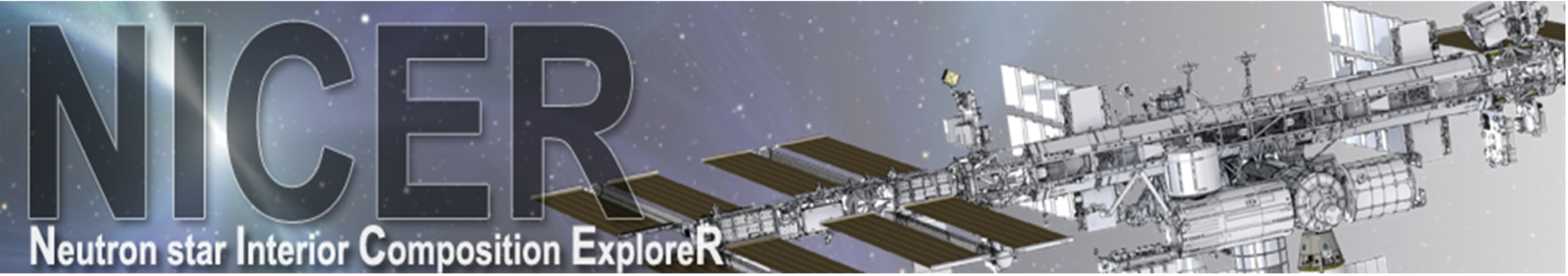

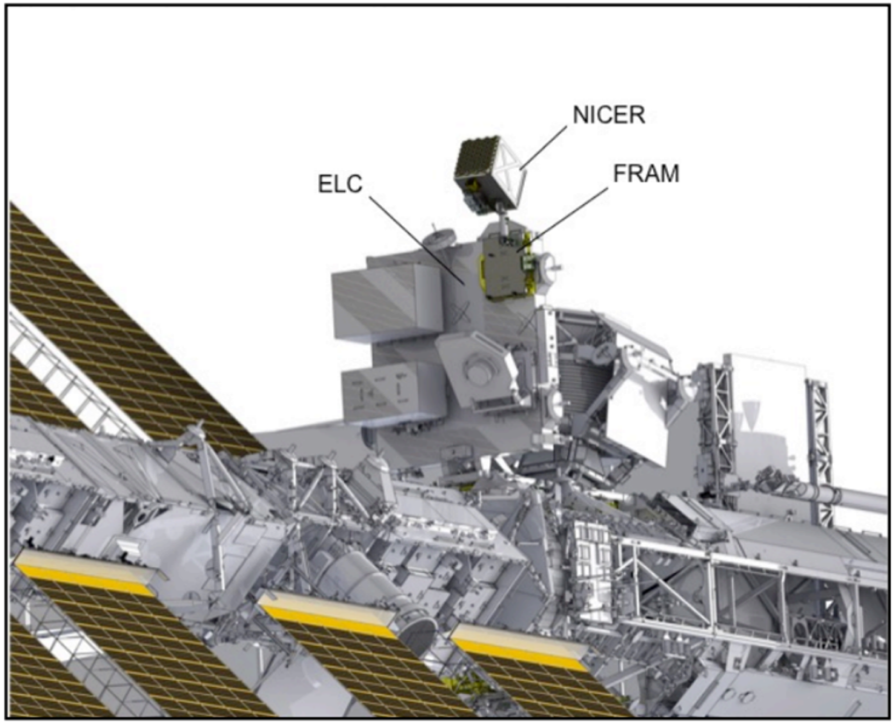

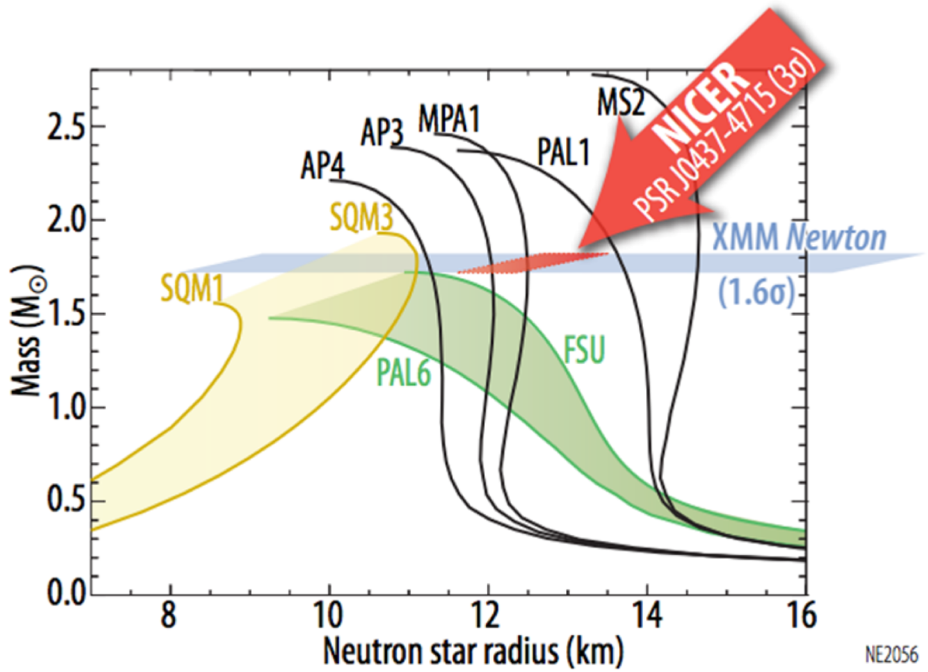

NICER 2017

Gendreau, K. C., Arzoumanian, Z., & Okajima, T. 2012, Proc. SPIE, 8443, 844313

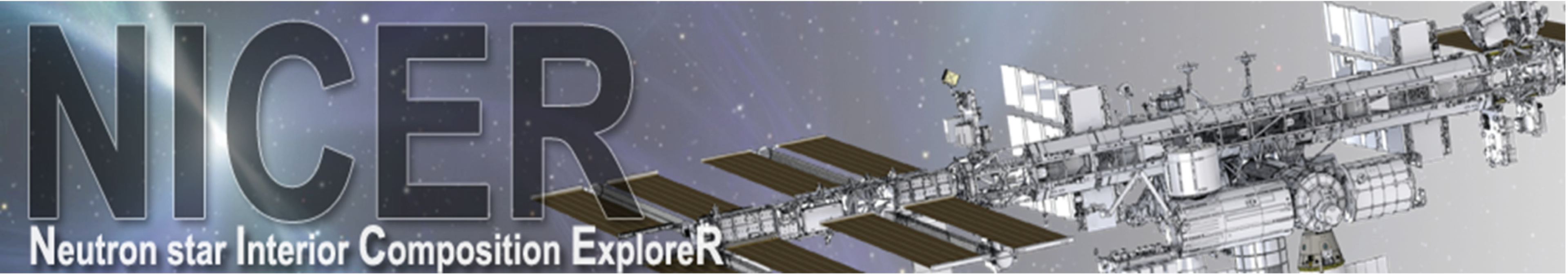
NICER
Neutron star Interior Composition ExplorerR

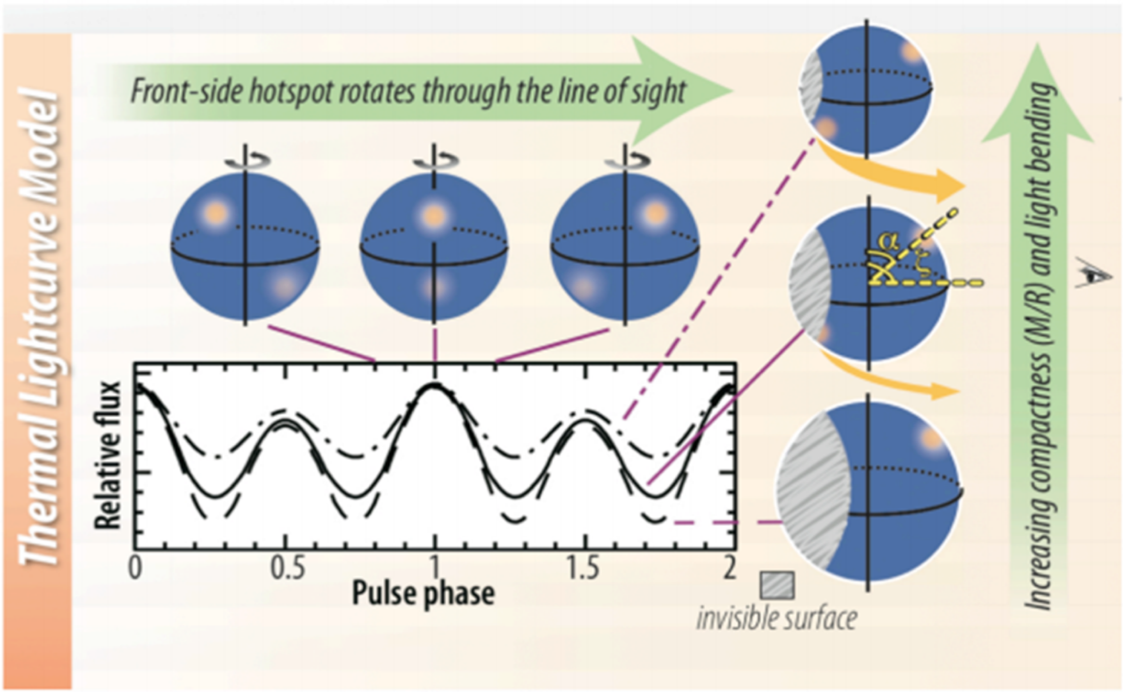
Thermal Lightcurve Model
Front-side hotspot rotates through the line of sight
Increasing compactness (M/R) and light bending
Relative flux
Pulse phase
0
0.5
1
1.5
2
invisible surface

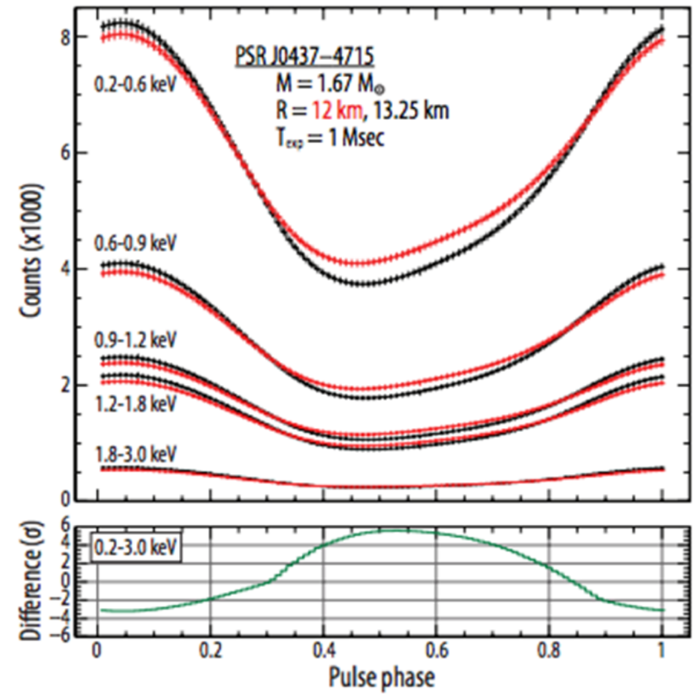
PSR J0437−4715
M = 1.67 M⊙
R = 12 km, 13.25 km
T_exp = 1 Msec
0.2-0.6 keV
0.6-0.9 keV
0.9-1.2 keV
1.2-1.8 keV
1.8-3.0 keV
Counts (x1000)
0.2-3.0 keV
Difference (σ)
Pulse phase

Hot Spots

Implications from GW170817
Nonlocal NJL

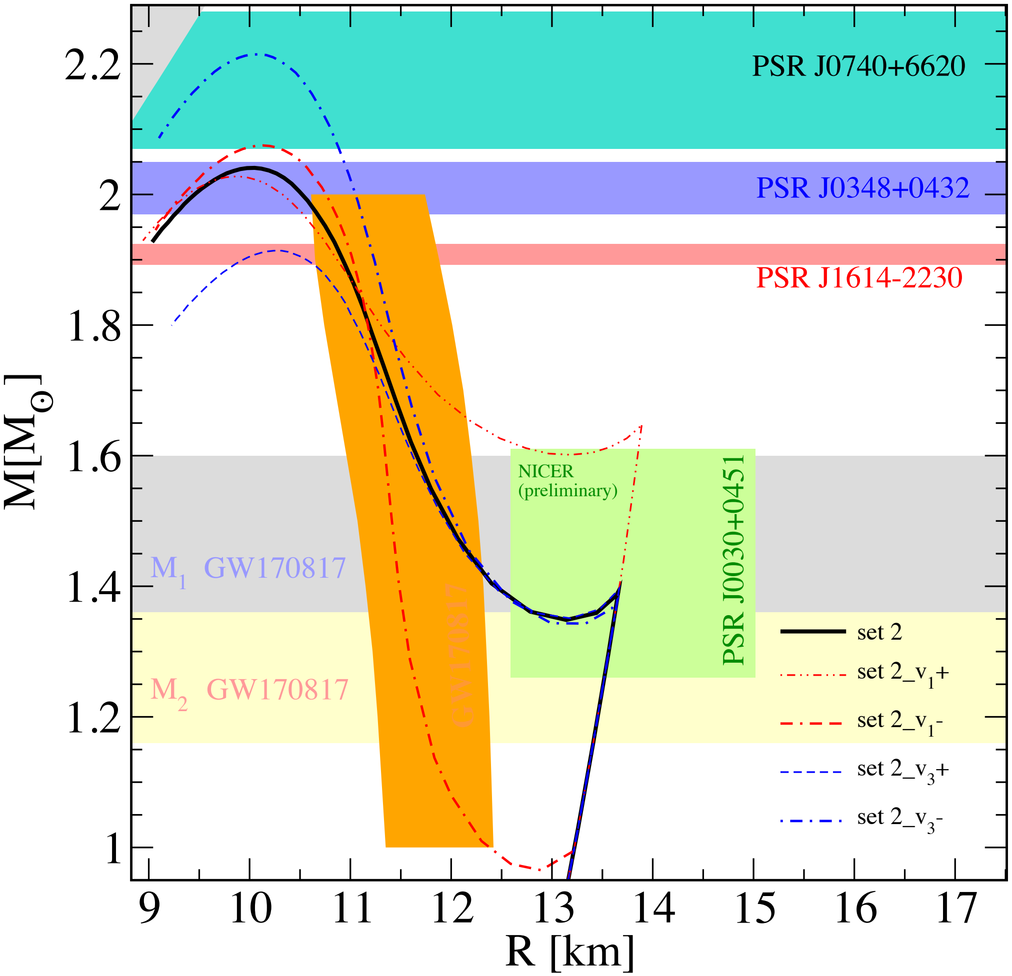

D. Alvarez-Castillo, D. Blaschke, G. Grunfeld, V. Pagura
Phys. Rev. D 99, 063010 (2019) - arXiv: 1805.04105

Implications from GW170817
Nonlocal NJL

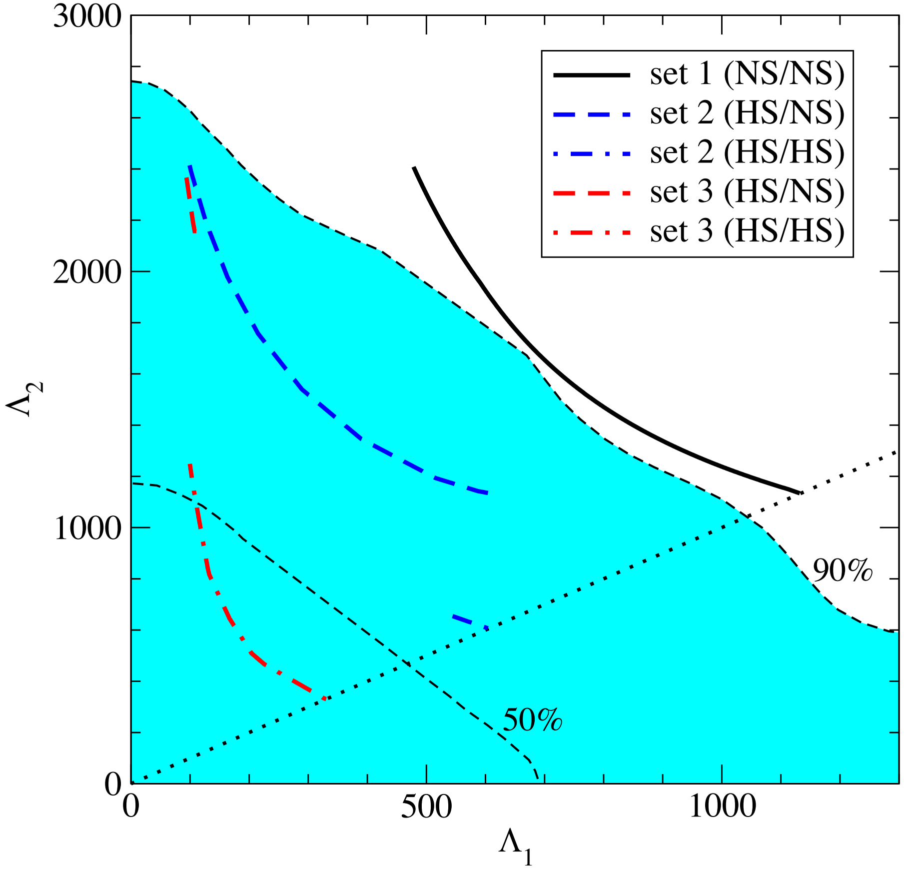

D. Alvarez-Castillo, D. Blaschke, G. Grunfeld, V. Pagura
Phys. Rev. D 99, 063010 (2019) - arXiv: 1805.04105

Gravitational Wave Signals

First Order Phase Transitions

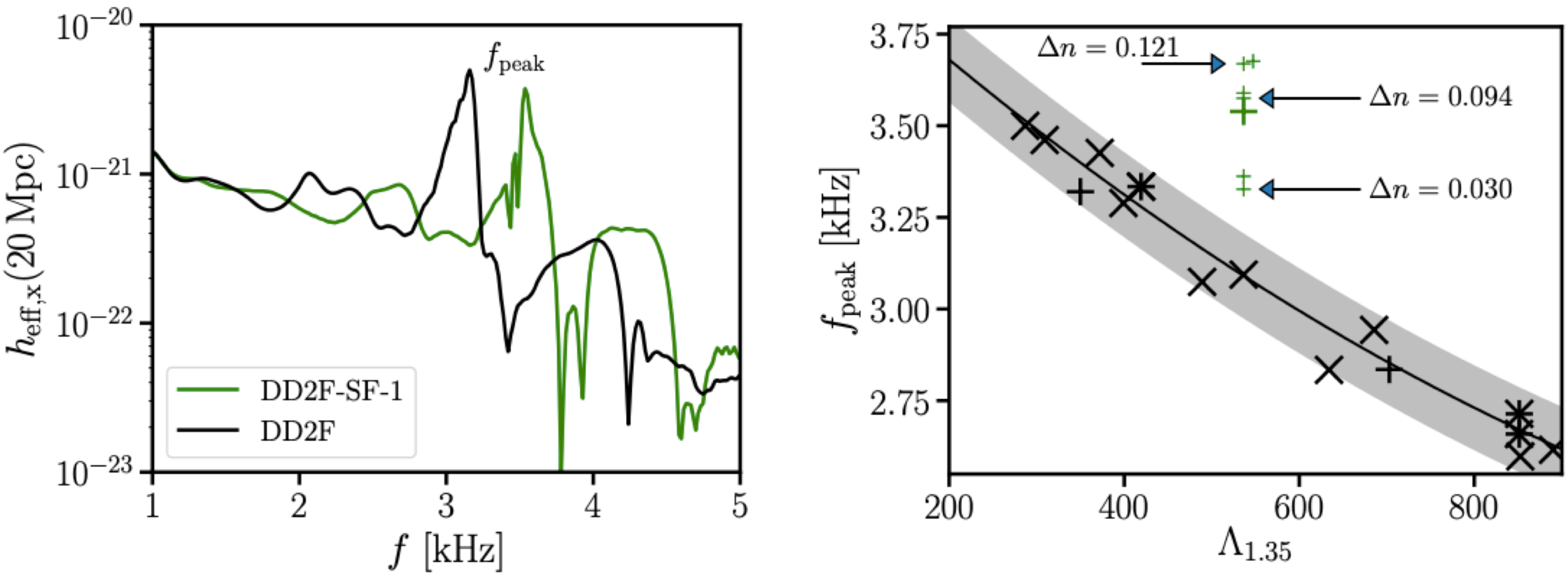

A. Bauswein et al. - arXiv: 1904.01306, PRL 122 (2019) 061102

Chapter 1

Astrophysical aspects of general relativistic mass twin compact stars

1.1 Introduction

Compact stars, the stellar remnants following the death of main sequence stars, have been the subject of investigation since the beginning of the last century. In particular, the determination of the internal composition of neutron stars is an open problem. Researching it involves many areas of physics, like nuclear, plasma, particle physics and relativistic astrophysics. Moreover, due to the enormous compactness (as expressed in the mass-radius ratio) of compact stars, these objects are extremely relativistic. Therefore, one can neither exclusively apply non-relativistic quantum mechanics nor classical Newtonian gravity to describe the observational properties of compact stars.

NICA Complex

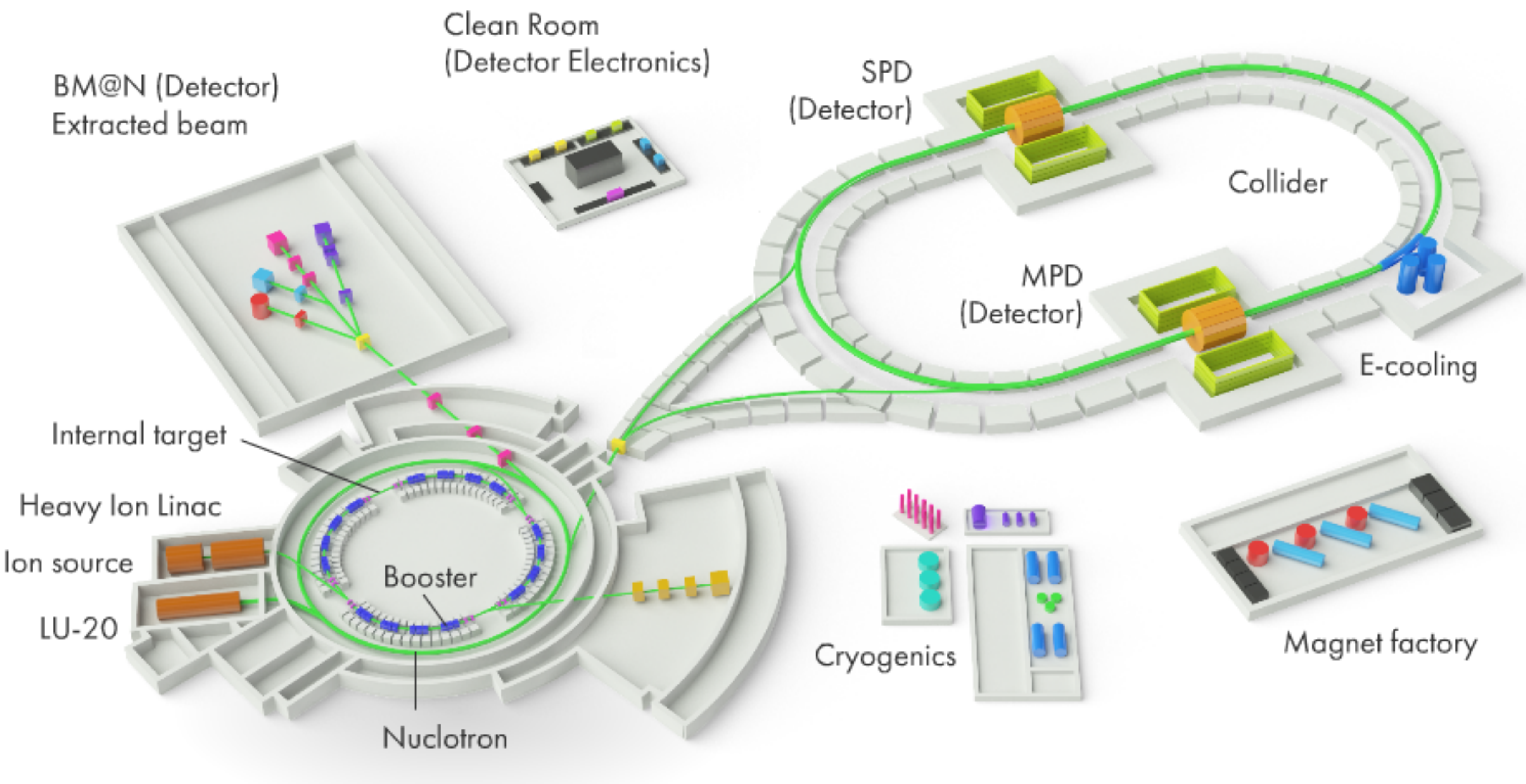

NICA Collaboration Map

Australia
Azerbaijan
Armenia
Belarus
Bulgaria
Brazil
Vietnam
Germany
Greece
Georgia
India
Italy
Kazakhstan
China
DPRK
Mexico

Moldova
Mongolia
Poland
Romania
Russia
Serbia
Slovakia
USA
Czech Republic
Ukraine
Uzbekistan
France
SAR
Japan
CERN

updated 04.05.2019

MexNICA Collaboration

Main Goal

To contribute in the study of the QGP phase diagram (CEP)

- To study, from the theoretical point of view, the mechanism responsible for the restoration of chiral symmetry and to study the QCD phase diagram at finite values of temperatura and density.

- To study, from the experimental point of view, signatures that allow to locate the CEP and contribute to the MPD collaboration with a detector (BEBE) for increasing the pseudorapidity acceptance, optimization of event plane resolution and trigger system.

IWARA 2020

9th International Workshop on Astronomy and Relativistic Astrophysics

Palacio de Minería, Mexico City, Mexico

6 – 12 September, 2020

https://indico.cern.ch/event/iwara2020/

iwara2020@gmail.com

Local Organizing Committee
Alfredo Macías, UAM, Mexico
Dany P. Page Rollinet – UNAM, Mexico
Darío Nuñez, ICN-UNAM, Mexico
Enrique López, FC-UNAM, Mexico
Gabriella Piccinelli – FES Aragón, UNAM, Mexico
Luis A. Ureña – UG, Mexico
Mariana Vargas Magaña – UNAM, Mexico
Peter O. Hess – UNAM, Mexico, Chair
Roberto Sussman – UNAM, Mexico
Tonatiuh Matos – CINVESTAV, Mexico

Organizing Committee
Alfredo Macías, UAM, Mexico
Aurora Pérez Martínez – ICIMAF, Cuba
Bruna C. Folador – UFRGS, Brazil
Carlos Javier Solano Salinas – UNI, Peru
César Zen – UFRGS, Brazil – Co-Chair
Dany P. Page Rollinet – UNAM, Mexico
Darío Nuñez, ICN-UNAM, Mexico
Dimiter Hadjimichef – UFRGS, Brazil
Elena Bratkovskaya – FIAS/JWGU, Germany
Enrique López, FC-UNAM, Mexico
Gabriella Piccinelli – FES Aragón, UNAM, Mexico
Hugo Pérez Rojas – ICIMAF, Cuba
Joerg Aichelin – SUBATECH, France
Jorge Horvath – IAG/USP, Brazil
Luis A. Ureña – UG, Mexico
Magno Machado – UFRGS, Brazil
Mariana Vargas Magaña – UNAM, Mexico
Milton R. Gamarra – UNSAAC, Peru
Moisés Razeira – UNIPAMPA, Brazil
Peter O. Hess – UNAM, Mexico, Chair
Ricardo G. Felipe – ISEL/IST, Portugal
Roberto Sussman – UNAM, Mexico
Thomas Boller – MPE, Germany
Tonatiuh Matos – CINVESTAV, Mexico

IWARA
From Quarks to Cosmos

International Advisory Committee
Carola Dobrigkeit – UNICAMP, Brazil
Christian Motch – CNRS, France
David Blaschke – UWr, Poland
David E. Alvarez-Castillo, JINR, Russia
Débora Peres Menezes – UFSC, Brazil
Eduardo Guendelman – BGU, Israel
Ernesto Kemp – UNICAMP, Brazil
Félix Mirabel – IAFE/CONICET, Argentina
Fridolin Weber – SDSU, USA
German Lugones – UFABC, Brazil
Helio T. Coelho – UFPE, Brazil
Horst Stoecker – GSI, FIAS & JWGU, Germany
Ignatios Antoniadis – CERN, Switzerland
Ignazio Bombaci – UNIPI, Italy
José A. de Freitas Pacheco – OCA, France
Manuel Malheiro de Oliveira – ITA, Brazil
Marcelo Chiapparini – UERJ, Brazil
Marcelo Gleiser – Dartmouth College, USA
Marcus Bleicher – HIC for FAIR, Germany
Massimo Della Valle – AOC, Italy
Norberto Scoccola – Tandar/CNEA, Argentina
Norman K. Glendenning - LBNL, USA
Paolo Giommi – ASDC/ASI, Italy
Pascal Chardonnet – US, France
Remo Ruffini – ICRANet, Italy
Renxin Xu – PKU, China
Rosana de Oliveira Gomes – FIAS, Germany
Sergei B. Popov – SAI/MSU, Russia
Sergio B. Duarte – CBPF, Brazil
S. O. Kepler – UFRGS, Brazil
Thaisa Storchi Bergmann – UFRGS, Brazil
Tsvi Piran – HU, Israel
Ulisses Barres de Almeida – CBPF, Brazil
Valdir B. Bezerra – UFPb, Brazil
Veronica Dexheimer – KSU, USA

Conclusions

- USEC conjecture has been corroborated and E_s related quantities found to be correlated with the NS radius.
- GW170817 favours softer EoS and together with the Durca constraint DD2F-like EoS are favoured. Hybrid stars with strong first order transition are also favoured.
- Future GW observations, NICER and SKA will soon result into stronger NS EoS constraints.
- Many possible astrophysical scenarios for mass twins could be confirmed implying a CEP in QCD.

Gracias